#79018
#82035

Structure and Stratigraphy of the Western Florida Shelf

Part I

Multichannel Reflection Seismic Data

by

Ball, M. M.[1]; Martin, R. G.[2]; Foote, R. Q.[3];
Applegate, A. V.[4]

Open-File Report 88-439

[1]USGS Woods Hole, MA
[2]Elf Acquitaine Petroleum, Houston, TX
[3]USGS Corpus Christi, TX
[4]Florida Bureau of Geology, Tallahassee, FL

This report is preliminary and has not been reviewed for conformity with U.S. Geological Survey editorial standards and stratigraphic nomenclature.

INTRODUCTION

This paper presents a synthesis of multichannel seismic data on the Western Florida shelf (Fig. 1). This work is part of an ongoing regional program conducted by the U.S. Geological Survey in studying the Exclusive Economic Zones of the United States.

The data include 1270 km of 32-fold, common-depth-point (CDP), reflection seismic line obtained with a 3200 m, 64 channel, hydrophone streamer and a 2000 in^3 airgun array. The rationale for the line layout was to tie eight key exploration wells among the 14 existing in federal waters prior to 1980 to 4 key wells in Florida. An attempt was also made to connect our survey with that of the University of Texas Institute of Geophysics in the deep Gulf of Mexico basin. A second set of 1500 km of 24-fold CDP data were collected using a 1200 m, 24-channel streamer and a 550 in^3 airgun source. This set was intended to tie additional wells, drilled between 1979 and 1983, and to infill our original net. Gravity and magnetic measurements were also made along these lines.

Our subsurface information in federal waters consists of well logs and files released to us initially by the Conservation Division of the U.S. Geological Survey and subsequently by the U.S. Minerals Management Service. Most information from wells in state waters was provided by the Florida Geological Survey.

Table 1 lists wells included in our study and summarizes the types of logs and other information available from each well. Spontaneous potential or gamma ray, resistivity or conductivity, sonic and density logs were generally available. Lithologic information, paleontologic and log picks on stratigraphic units and dip-meter data were also common. Check shot surveys for velocity analysis were available in three wells.

Table 1

Operator	Lease	Block	Well No.	Location Lat.N	Location Long.W	Sea Level Datum Total Depth Ft.	Sea Level Datum Total Depth M.	Information Available	Water Depth (Ft.)	Elev. (Ft) Kelly Bushing
Gulf	2468	360	1	29°35.7	87°25.6'	20,870	6361.2	SPDIL, S, GD DM, PT	236	90
Exxon	2486	162	3	29°50.2'	86°19.6'	17,855	5442.2	SPDIL, S, GD ND, PT, VCSS	258	83
Amoco	2502	31	1	29°56.5'	86°16.7'	18,242	5559.9	SPDIL, S, DM, L	128	96
Sun	2490	166	1	29°48.5'	86°04.8'	17,521	5340.5	SPDIL, S, GD DM, L, PT	142	87
Calco	Fl.St.224A		2	29°47.1'	84°22.9'	10,526	3208.2	SPDIL, PT	30	35
Texaco	2516	252	1	28°41.7'	84°19.8'	15,582	4749.4	SPDIL, S, GD ND, DM, PT, VCSS	126	84
Coastal Ragland	Fl. Permit No. 66		1	29°08.1' Levy Co. Florida (Sec. 16, T15S, R13E)	82°59'	5,836	1778.7	SPR, L, PT	—	14
Shell	2527	7	1	27°57.1'	83°41.9'	18,371	5599.6	SPDIL, ND, L, PT	125	81
Texaco	2523	100	1	27°50.4'	83°25.8'	17,304	5274.3	SPDIL, ND, L PT, VCSS	98	84
Calco	Fl.St.224B		3	28°05.5'	82°52.8'	10,524	3207.6	SPIE, S, ND, PT		
Mobil	3344	566	1	27°23.6'	84°03.1'	15,782	4810.4	SPDIL, S, GD, ND DM, T, PT	220	89
Mobil	3341	915	1	27°03.5'	84°12.5'	18,040	5498.3	SPIE, S, GD, ND DM, PT	370	88
Shell	3912	265	1	26°39'	83°57'	12,261	3737	SPDIL, GD, ND DM, PT	324	72
Mobil	3903	654	1	26°18'	84°05.5'	10,077	3071.3	SPDIL, S, ND GD, DM, PT	455	73
Odeco	3909	188	1	26°44.4'	83°27.1'	11,145	3396.8	SPDIL, ND, GD DM, PT	180	95
Tenneco	3917	672	1	26°17.5'	83°23.8'	11,090	3380	SPDIL, ND, GD, DM, L, PT	190	90
Calco	Fl.St.224B		1	26°41.1'	82°19'	13,936	4247.5	R, PT	15	39
Mobil	Fl.St.224B		1			12,910				21

Abbreviations used in summarizing log types are as follows:
SPDIL, Spontaneous Potential Dual Induction Laterolog; S, Sonic; GD, Gamma Density; ND, Neutron Density; VCSS, Velocity Check Shot Survey; DM, Dip Meter; PT, Paleontologic Tops; SPIE, Spontaneous Potential Induction Electric; T, Temperature.

We have used sonic and density logs to create synthetic seismograms at well sites to achieve the best possible tie of CDP profiles to subsurface data. Where possible, integrated sonic logs together with velocity surveys were used to arrive at time-depth conversions. Away from these sites, stacking velocity analyses were used to arrive at depth conversions to key stratigraphic horizons.

Our report begins with a brief description of the acquisition and processing systems used to generate our seismic data. Then we describe our seismic lines (Fig. 1) and their implications relative to the geologic history, structure and stratigraphy of the Eastern Gulf of Mexico Region. The description and discussion fall more or less naturally into a geographic organization dictated by the conclusions of Klitgord and others (1984) regarding structural features of Florida and the Western Florida Shelf region (Fig. 2) that were accepted by us as an initial working hypothesis.

Working primarily with potential field data, Klitgord and others (1984) envisioned a set of fracture zones crossing South Florida and the Western Florida Shelf in a northwesterly direction. During the Late Jurassic opening of the Gulf of Mexico, these faults connected the Gulf and Atlantic spreading centers and accommodated Gulf opening by acting as a colossal tranform zone in the sense that the zone formed in the offset between two regions of spreading. The concept is complicated by the existance of blocks of pre-Mesozoic crust within the transform zone. These blocks were thought to be separated by zones of extension or spreading underlain either by extensively rifted transitional crust or Jurassic, possibly oceanic crust. This oceanic crust, if present, is aberrant in that it is thick and lacks the magnetic stripes (seafloor-spreading anomalies) usually associated with oceanic crust. The regional tectonic units within and bounding the tranform zone are shown in Figure 2. From northwest to southeast, those included on the Western Florida Shelf are the Apalachicola Basin, the Middle Ground Arch, the Tampa Basin, the Sarasota Arch and the South Florida Basin. Our descriptions and discussions are grouped according to these structural provinces.

Main conclusions of our study are that (1) the crust beneath the Western Florida Shelf is esentially continental, (2) the granite high beneath the central shelf known as the Sarasota Arch rivals or surpasses the Forida Peninsular Arch in magnitude and (3) tectonic activities controlling distribution of Florida basement features are Late Paleozoic as well as Early Mesozoic in age.

EQUIPMENT

Two seismic systems were used to obtain the geophysical data on which this study is based. In August 1979, the M/V SEISMIC EXPLORER of Seismic Explorations International (SEI), under contract to the U.S. Geological Survey, ran 1270 km on the Western Florida Shelf (Fig. 1). In October 1982, aboard R/V GYRE of Texas A&M University, a group of U.S. Geological Survey personnel obtained an additional 1500 km of CDP, gravity and magnetic data (Fig. 1).

The main features of the SEI system were: a digital recorder with an instantaneous-floating-point gain constant of 24 dB, a 64 channel hydrophone streamer, 3200 m long, and a 21 airgun array with a total volume of 2000 in^3

and a pressure of 2000 psi. Sampling interval was 4 msec. Record length was 8 sec. The distance from the center of the airgun array to the center of the farthest phone group was 3338 m and 188 m to the nearest phone group. Shot points were 50 m apart to obtain a 32-fold stack. Navigation was by an integrated satellite-loran-doppler-sonar-system.

The SEI data were processed by Geophysical Data Processing Center Inc. of Houston, Texas. Processing procedures were standard with the exceptions that: (1) A deringing deconvolution with a 128 msec operator length was done prior to stacking. (2) A time-variant predictive deconvolution with a filter operator length of 100 msec and automatic picking of the second zero-crossing was applied after stacking to futher suppress multiple energy. (3) Velocity analyses were performed every 3 km using a technique that included determination and consideration of amount and direction of apparent dip. (4) Automatic gain ranging with a 750 msec window was applied during processing. (5) Lines affected by sloping seafloor were deconvolved before stacking and time variant filter parameters adjusted to follow the seafloor geometry.

The system used aboard R/V GYRE consisted of a digital recorder, a 24 channel hydrophone streamer, 1200 m long, and a 500 in^3 airgun with firing pressure at 1800 psi. Sampling rate was 2 msec. Record length was 4 sec. The distance from the gun to the center of the far phone group was 1390 m and to the center of the near phone group was 240 m. Shot points were 25 m apart to obtain a 24-fold stack. An integrated satellite-loran-doppler sonar-system supplied navigation. The USGS's data-processing group in Denver, processed these CDP data according to standard procedures.

The data taken with the 3200 m streamer and 2000 in^3 airgun array, aboard M/V SEISMIC EXPLORER (Arabic numerals, Figure 1) are vastly superior to those obtained on R/V GYRE using a much smaller streamer and source (Roman numerals, Figure 1). The former consistently show coherent primary events from within the units underlying the Mesozoic section on the Western Florida Shelf while the latter tend to do so only in the inshore area of the Middle Ground Arch (Fig. 2), where pre-Mesozoic basement occurs at depths of less than 2 km.

REFLECTION SEISMIC DATA

General

We have compressed scales of many of our seismic reflection profiles in order to illustrate regional aspects of the geology of the Western Florida Shelf. Record sections at expanded scales are keyed to the regional lines and used to depict details of interest. Most time sections are plotted at a vertical scale that approximates, to ±30%, an exaggeration of 1 at the total depths of deep wells within the study area (20,000 ft or 6.1 km).

Unavoidable distortions remain; first, because of the increase in velocity with depth; and second, because of a positive regional velocity gradient, from northwest to southeast, due to the post Paleozoic section's loss of its marly, shaly character and change to dense limestone, dolomite and anhydrite. For example, in the Apalachicola Basin (Figure 2), in the northwest part of the study area, the interval velocity in the upper second of reflection time is about 7000 ft/sec (2.2 km/sec); from one to two seconds, interval velocity is about 10,500 ft/sec (3.2 km/sec) and in the interval from 2 to 3 seconds, it is approximately 12,900 ft/sec (3.9 km/sec). From these

relationships it follows that vertical exaggeration in the upper second in this area is approximately 50% greater than in the next second and about twice that of the third second of reflection time. To the southeast, on the Middle Ground Arch (Figure 2), where post Paleozoic section has a time dimension of slightly more than 2 seconds, the interval velocity in the upper second is 12,500 ft/sec (3.8 km/sec); and in the next second, 13,100 ft/sec (4 km/sec). It follows that there is little variation of vertical exaggeration in the post-Paleozoic in time sections in this region and that this exaggeration roughly equals that of interval from two to three sec in the Apalachicola Basin. Over these interval velocity ranges of 2 to 4 km/sec, allowing for the mean data frequency of 20 Hz, a single cycle represents from 50 to 100 m of section.

Age assignments shown in the margins of seismic sections and structural cross sections are based on the ties of our seismic profiles to various key wells shown in Figure 1. The accuracy of these ties depends on the paleontologic and e-log picks in the wells and the conversion of reflection time to depth necessary to match a given reflection to the depth of a given stratigraphic horizon in the tied wells.

Stratigraphic correlations and terminology used in this paper are shown in table 2. This table represents an attempt to reconcile the terminology used by the Mineral Management Service in the Florida Panhandle with that of Addy and Buffler (1984) at Destin Done and the Florida Geological Survey in South Florida.

Apalachicola Basin

The 250-km-long strike line (Fig. 3) includes Lines 1-3 and the western end of Line 8 (Fig. 1) and connects the Gulf well, G2468, on the west; through the Exxon well, G2486, and the Sun well G2490 to the western flank of the Middle Ground Arch on the east. The salient features of this line are: 1) the Gulf 2468 structure (Figs. 3 and 4); 2) the Destin Dome (Figs. 3 and 5); and 3) the basement fault (Figs. 3 and 6) 6.5 km east of the Sun well.

On the east, the Gulf structure's eastern flank appears to be onlapped by pre-Cretaceous sediments (Fig. 4). There is slight thinning over the structure in latest Jurassic (Cotton Valley) time, and oldest Cretaceous (Hosston time). Positive structural expression of this feature ceases by the end of Early Cretaceous time. The east flank of the structure spans 15 km. A clear, continuous and slightly depressed basement reflection underlies the

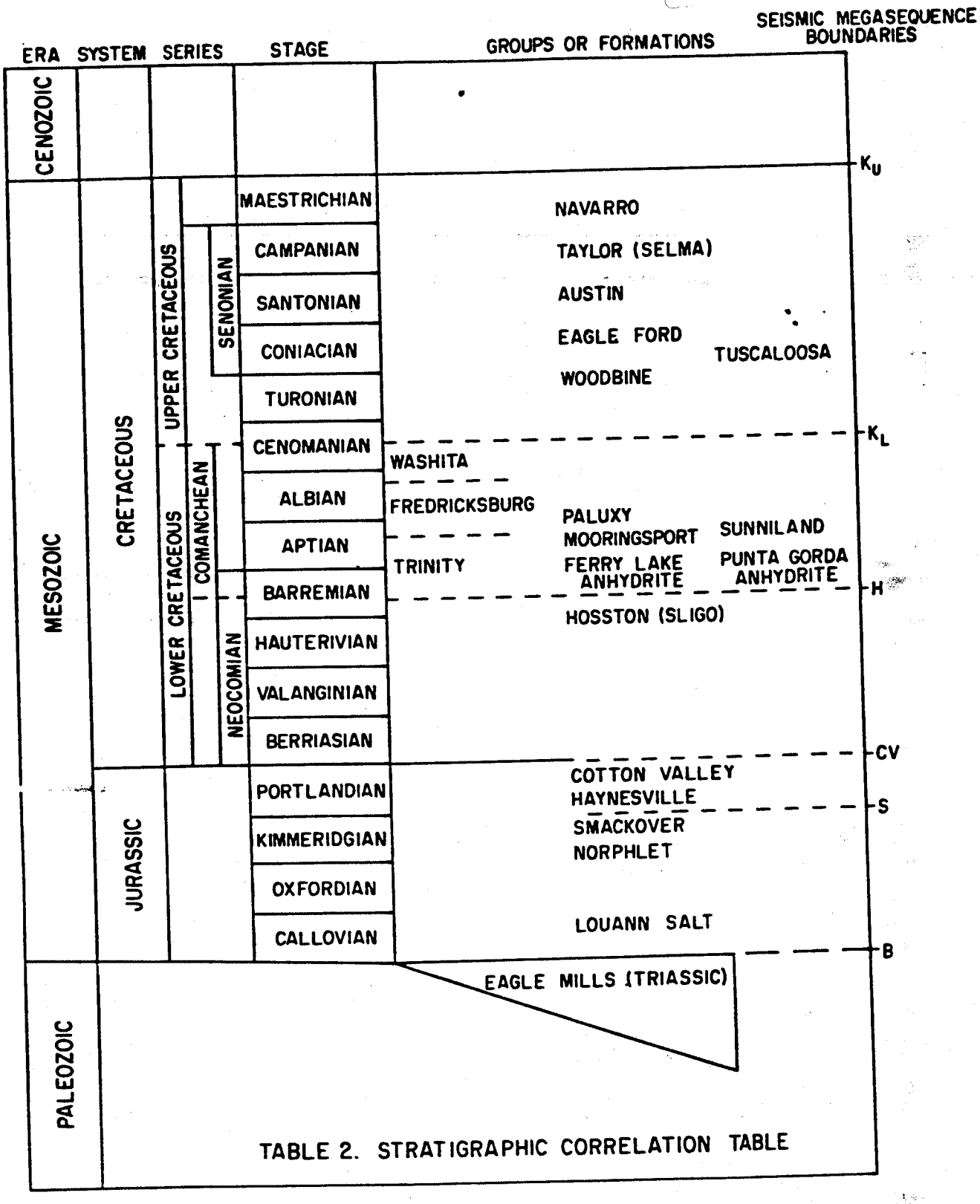

TABLE 2. STRATIGRAPHIC CORRELATION TABLE

Gulf structure and breaks up eastward beneath the structure's eastern flank (Fig. 4). The depression may result from a velocity decrease in the core of this structure relative to laterally adjacent section. The fact that the inferred basement surface passes beneath the shallower structural crest with slight negative relief, reinforces the likelihood that this feature may be a salt swell or pillow, because salt with its interval velocity of 4.5 km/sec, is slow relative to the 6 km/sec interval velocities encountered near the base of the Gulf well. Dip changes and diffractions indicate possible faults cutting the basement and continuing upward into Cotton Valley and older Jurassic sedimentary rocks (Fig. 4). Depending on an interpretor's choice of correlations across this fault zone, it is possible that major offsets of the Jurassic-basement contact attend the faulting. Intrabasement reflections dip toward the west with apparent dips approaching 10 degrees (Fig. 4). Positive relief midway between the Gulf and Destin structures on the Hosston reflection and continuing upward into Cenozoic section (Figure 3) is probably due to depositional upbuilding.

The Destin Dome (Fig. 3) has an apparent extent of about 90 km. The growth history of this structure, as revealed on its western flank (Fig. 3), appears to begin in youngest Early Cretaceous and continue through Late Cretaceous and Cenozoic time. A discernable band of reflections marks the contact of the inferred base of Jurassic sedimentary section and the underlying salt. This reflection band is labeled "S" (Fig. 3), for Smackover in our records with the realization that its duration in time spans density and velocity contrasts within the basal Haynesville, Smackover, Norphlet and upper salt section. On this strike line, the minimum positive relief of closure on the S reflection band occurs on the Destin Dome's eastern flank (Fig. 3) and measures about 500 m (1500 ft). Apparent fills of reflection sequences within this reflection band are visible in expanded record sections (Fig. 5). These fills have time durations measured in tenths of seconds and could represent substantial thickness variations of more than 100 m in sedimentary units of the basal Jurassic Smackover and Norphlet formations. An essentially flat basement reflection (Fig. 3) continues beneath the Destin Dome. Lack of relief on this basement reflection and the occurrence of salt at the base of both the Exxon and Sun wells provide the basis for identifying the Destin Dome as a salt swell. The absence of velocity pull-down on the basement surface occurs because the velocity of materials laterally adjacent to the salt more or less equals salt velocity. The basement reflection fades as the inferred salt interval thins eastward toward the Sun well (Fig. 5). Some faulting is indicated by terminations and dip changes at the basement surface continuing upward into Jurassic sediments (Fig. 5).

East of the Sun well, a major fault (Fig. 6), downthrown to the west, with a throw of at least 1000 m cuts the "S" reflection band and continues upward into the Oldest Cretaceous, Hosston section. No clearcut reflection is associated with the salt-basement contact at this position. Eastward from this fault, a few weak discontinuous reflections may mark the salt-basement contact (Fig. 3); as the salt thins eastward on the western flank of the Middle Ground Arch, these reflections appear to die out or merge with the overlying reflection band marking the basal Jurassic sedimentary section.

Dip lines 4, 5 and 6-7 (Fig. 1), over the Destin Dome crest (Figs. 7-11), show its north-south dimension exceeds 30 km (20 mi.). Growth history, although somewhat obscurred by regional northward thinning, appears to span

latest Early Cretaceous to Cenozoic time (Fig. 7). The thick band of reflections marking impedance contrasts in the earliest Jurassic sedimentary rocks and at the salt-sedimentary rock contact is the deepest reflection horizon that shows the domes positive structural relief (Figs. 7-9). Minimum relief of structural crest on this horizon occurs on the northern flank (Fig. 9) and measures about 500 m (1500 ft). An essentially planar, salt-basement reflection dips southward, at an angle of 3 degrees, beneath the Dome (Figs. 7-9, 11). This regional dip contributes to the dome's asymmetry by oversteepening the south flank and opening closure on the north.

Two scales of faulting are evident in the dip lines (Figs. 7-11). The older fault system lies just updip from the Destin Dome and displaces latest Jurassic sedimentary rocks on down-to-the-north faulting that cuts upward into the oldest Cretaceous (Hosston) section (Figs. 7, 8, 9 and 11). Accentuated southward dips and thickening in the fault zone indicate major north-dipping faults with suggestions of south-dipping subsidiary faults and concentration of activity during Late Jurassic time. The salt-basement reflection fades toward and is not apparent north of this deep faulting. A smaller scale fault system disrupts shallower horizons over the seaward crest of the Destin Dome (Figs. 7, 8, 9 and 11). The faults are reminiscent of extensional features on salt dome crests where downdropped keystone blocks overlie horsts bounded by the same faults after they cross at greater depth. These faults fade with increasing depth and none of them appear to offset the Late Jurassic, "S" reflection. These faults appear to cut almost to the seafloor on Lines 4 and 6-7 (Fig. 8 and 11).

A deep, older anticlinal feature lies 30 km south of the Destin Crest on line 6-7 (Figs. 7 and 10). Thinning over this feature is concentrated in the Neocomian section (Hosston). Maximum structural relief is about 500 m on the uppermost Jurassic, Cotton Valley. The structural relief diminishes above the Cotton Valley and dies out in the Upper Cretaceous. The apparent breadth of the structure in our crossing is about 6 miles (10 km). A pinchout of section in the lowest Jurassic sedimentary rock-salt top interval is indicated on the north flank of the structure (Fig. 10). A flat, inferred salt-basement reflection (Fig. 10) dips southward 3 degrees beneath the structure. Lack of basement relief beneath the structure again argues for identification of this feature as a salt swell. Southward dipping, intrabasement reflections beneath the structure's north flank (Fig. 10) are probably real and reflect an angular unconformity at a peneplained basement surface.

The Middle Ground Arch

Two characteristics distinguish the western flank of the Middle Ground Arch, revealed on the 220-km-long strike line connecting the Sun G2490 well and the Texaco G2516 well (Line 8, Figs. 1, 12 and 13). The first is the continuous, planar reflection character of the Late Jurassic and younger sedimentary rock section as it thins toward the arch crest. Most of the apparent thinning results from velocity increase of this Mesozoic-Cenozoic section. Some thinning results from the line orientation being slightly updip toward the southeast on basement structure. There is however a real loss of section by pinch-out and onlap of the Jurassic rocks onto a broad basement nose whose axis dips gently southwestward beneath the Texaco G2516 well. Of the Late Jurassic section, only the uppermost Cotton Valley remains at the Texaco well where it has thinned to 400 m from a thickness of about 750 m in

the Sun well. The Cotton Valley top in the Texaco G2516 well is at 3835.5 m subsealevel and is 65 m lower than the Cotton Valley picked at the Sun well. The basement penetrated at 4316 m below sealevel consists of 433.7 m (1423 ft) of grey siltstone identified as Paleozoic in age based on palynologic studies (Gee and others, 1976). The upper 30 m of this Paleozoic section is a conglomeratic, sandy, red siltstone with a noticeable admixture of mica, chlorite and metamorphic fragments (Gee and others, 1976). The local structure tested by the Texaco well has almost indiscernable relief at the southeastern end of Line 8 (Fig. 12). The second distinguishing characteristic of the reflection data along this line is the variability of the band of reflections marking the contrasts between Jurassic sedimentary rocks and the underlying basement. Toward the west, across the 75 km expanse between the fault east of the Sun well (Fig. 12) and a slight basement monocline (Figs. 12, 13), this reflection band is generally planar and distinct. An exception is a 15 km broad zone of broken reflections (Figs. 12, 14). This zone appears to result from basement topography related to faulting extending upward into the Cotton Valley section that is accompanied by slight positive basement relief with horizontal extents of 2 to 3 km that protrude 100 m or so upward into the Jurassic sedimentary rocks. Margins of these basement highs are attended by numerous diffractions (Fig. 14). Material between the highs lacks seismic impedance contrast with the overlying Jurassic sedimentary rocks. Southeast of the basement monocline (Figs. 12, 13), the distinctive character of the basement reflection is lost as this event becomes intermittent and indistinguishable in terms of reflection strength from reflections in the overlying Jurassic and Neocomian sections. This change in reflection character may mark the pinchout of Smackover and older Jurassic sedimentary rocks on the monocline's flank. Farther to the east, where no marked contrast between the Jurassic sedimentary rock and the basement is evident, one must conclude that the Jurassic section overlies Paleozoic rocks, similar to those below the Mesozoic-Paleozoic contact in the Texaco G2516 well at the southeastern end of line 8 (Fig. 12). Velocity and density variations within this rock sequence are insufficiently different to give rise to high-amplitude reflections. Small faults appear to offset and terminate reflections in the Jurassic section and in underlying Paleozoic basement.

The southeastward continuation of this strike line (Figs. 1, 15; Lines 13 and 14) shows a gently dipping basement reflection deepening down the southeastern flank of the Middle Ground Arch. The Mesozoic-Cenozoic section is characterized by essentially planar reflections with good continuity in the Jurassic and Lower Cretaceous units. An especially well-defined reflection occurs near the Aptian-Neocomian boundary around the top of the Hosston. Although appearing to be flat-lying, the reflections within the Upper Cretaceous and Cenozoic section are much less continuous than those they overlie. No marked contrast is generally visible at the Mesozoic-Paleozoic boundary, although some patches of resounding reflection character do occur (Fig. 15) that are similar to the short segments of high intensity reflection seen on the western flank of the Middle Ground Arch (Fig. 12, see Fig. 1 for location). The margins of these patches of strong reflectivity are sources of diffractions and intervening areas appear to be structurally high with very-low-relief drape reversals in the overlying Jurassic and Lower Cretaceous sedimentary rock section. Stratigraphic picks on Hosston and older units are somewhat lower in the Shell 2527 well, at the junction of Lines 13 and 14 (Fig. 1, 15), relative to the Texaco 2523 well at the southeast end of Line 14 (Fig. 1). The Shell well is slightly downdip. Little or no expression of an

updip extension of the Tampa Basin, located between the Middle Ground and Sarasota Arches (Fig. 2), is apparent on our strike lines 13 and 14 (Fig. 1).

Line VII (Fig. 1) is an updip strike line on the Middle Ground Arch that is noteworthy because it reveals an apparent graben (Fig. 16; see Fig. 1 for location). The graben, together with the Paleozoic basement tie at the intersection with Line 12 (Fig. 1) enables identification of the Mesozoic-Paleozoic boundary at updip locations over the extent of this line (Fig. 16). The flat-lying infill within the upper graben appears to onlap the deeper, southeastward-dipping and thickening, fill deposited during faulting (Fig. 16). If one accepts the apparent continuity of this upper flat-lying fill with intrabasement Paleozoic reflections toward the southeast, it follows that deposition of Paleozoic sediment postdates faulting, thus establishing evidence for earlier Paleozoic faulting and graben formation. The graben agrees in position with a northeast-trending gravity low and with a band of relatively short-wavelength magnetic anomalies on the profile along Line VII. The basement surface is essentially planar exhibiting some local highs as wide as five km with heights of less than 100 m. Line VII (Fig. 16) has been horizontally squeezed to accentuate the low-angle dips associated with structure along this line. Vertical exaggeration above the Paleozoic basement surface is approximately 4:1. The Paleozoic-Mesozoic boundary is also visible over short segments of Line VIII (Fig. 1).

The northeastern dip line on the Middle Ground Arch (Lines 9 and 10, Figs. 1, 17) reveals a great deal of structure on and within so-called basement rocks. At the northeast end of this line (Fig. 17), the Calco FL St. 224A well (Fig. 1, CA_2; Table 1) is projected into the end of the section from 2 miles to the northwest. This well is reported to have bottomed in the Triassic Eagle Mills Formation at 10526 ft (3208 m) below sea level (Applegate and Lloyd, 1985, p. 50). Jurassic spores are reported at 10290 ft (3136 m) below sea level and diabase was encountered at 10425 ft (3177 m) below sea level. Based on our time-depth conversion, the bottom hole depth agrees with a band of relatively high intensity, irregular and discontinuous reflections at 1.8 sec of reflection time (Fig. 17). This broken band of reflections continues 35 km toward the southwest to its termination on the seismic profile (Fig. 17). No deeper reflections are apparent below the northeastern half of this reflection band but the southwestern half is underlain by a strong band of reflections at about 3 sec (Fig. 17). This second band of reflections terminates on the southwest at about the location of the termination of the overlying reflection band (Fig. 17). Toward the southwest from the terminations of both the reflection packages, the deepest high amplitude reflection package occurs at 2.4 sec (Fig. 17). This reflection band begins where the others end and continues toward the southwest in a more or less continuous fashion to the intersection of line 8 (Figs. 1, 12). The strength of this reflection package varies considerably along the line with one particularly strong occurrence of a 3-km-long segment with a slight apparent northeastern dip (Fig. 17). A dip reversal is apparent at the intersection with line 8 (Fig. 17). This reversal has almost no expression at the level of the Hosston or top of Neocomian reflection (Fig. 17). This band correlates with the reflection package, marking the top of Paleozoic section, carried from the southeast on line 8 from Texaco 2516 (Fig. 1). Deeper, weaker reflections are visible over most of the extent of this reflection band.

It seems most likely that the shallow reflection band at 1.8 seconds on the northeast end of line 10 (Fig. 17) marks a level of concentration of Jurassic diabase sills in an Eagle Mills fill of a Triassic graben. The deeper reflection package at 3 sec (Fig. 17) may represent the contact of graben fill with underlying Paleozoic sedimentary rocks as reflections indicative of sedimentary section underlie the inferred Triassic-Paleozoic contact. The terminations of these two reflection bands (Fig. 17) and the initiation of a third reflection package that can be correlated with the Jurassic-Paleozoic boundary (Fig. 17) may mark the location of a down-to-the-northeast fault that forms one boundary of the Triassic graben. Throw on this inferred fault would be about 4500 ft or 1.4 km.

Southwestward from its intersection with line 8, line 10 (Fig. 17) reveals a continuous strong reflection at the Jurassic-Paleozoic boundary that separates the relatively low-amplitude but very continuous reflections in the overlying Jurassic section from the higher amplitude but much less continuous reflections below it. Throughout, the post-Paleozoic sedimentary section is distinguished by low angle, southwesterly dipping, continuous reflections of varying amplitudes. The post-Paleozoic section thins toward the northeast with onlaps and pinchouts apparent at its base. A possible intrabasement graben or basin fill is apparent over the southwesternmost 15 km of line 10 (Fig. 17).

Lines 11 and 12 (Figs. 1, 18) form an axial dip line on the Middle Ground Arch. These lines join at the Texaco 2516 well, (Fig. 1, Table 1) with line 11 downdip toward the southwest and line 12 extending updip toward the northeast. At the northeastern end of line 12, the Coastal Ragland No. 1 well (Fig. 1, C_R; Table 1) lies 25 miles to the northeast. Both wells bottomed in Paleozoic sediments. The Texaco 2516 well provides a reliable tie of stratigraphy to the seismic data down to the Jurassic-Paleozoic boundary. The reflections within the Jurassic and younger sedimentary section are typically continuous and converge toward the northeast. Pinch outs and onlap in a northeasterly direction are visible at the base of the Mesozoic section (Fig. 18).

The character of the reflection marking the Jurassic-Paleozoic boundary does not vary nearly as much here as it did over the northeastern half of line 10 (Figs. 1, 17). The basement surface is essentially a peneplain. Local relief is related to intrabasement structure and differential erosion. Structure in the overlying Mesozoic sedimentary section appears to be a result of drape over erosional basement highs. The positive feature at Texaco 2516 well is an example of one of these drapes. Relief of this structure is measured in tens of milliseconds on Jurassic and Early Cretaceous reflections and thus has a maximum vertical expression of around 100 m over a horizontal distance of 3 km. A major intrabasement high (Fig. 19) occurs beneath the northeastern end of line 12 at 4.4 sec. This time corresponds to a depth of approximately 13 km. Intrabasement reflections warp up over this feature and there is some apparent positive relief at the basement surface and in the overlying Mesozoic sedimentary rocks, which argues for a Mesozoic age for this structure. This feature may represent an intrusive igneous body.

Line VI (Figs. 1, 20) contains little useful information on the Jurassic-Paleozoic boundary. On the shelf, multiples obscure primary reflections below two seconds. The Cenozoic section is restricted to the upper second of

reflection time. An impressive sequence of basinward prograding reflections with as much as 0.5 sec of vertical relief make up a major portion of the middle to lower Cenozoic section (Fig. 21). The most useful portion of this profile occurs at and basinward of its crossing of the escarpment at the western edge of the Florida Platform.

Tampa Embayment

Seismic lines 15, 16, and 17 (Figs. 1, 22) form the longest dip line with reliable basement information. This profile lies between the relatively subdued, gently southwestward-dipping, nose on the regional Paleozoic-Jurassic peneplain known as the Middle Ground Arch and the Sarasota Arch (Figs. 1, 2). The line thus constitutes a dip line lying within the Tampa Embayment (Fig. 2). The updip, eastnortheast, end of line 17 (Figs. 22, 23) is ten miles (16 km) southwest of the Calco Fl. St. 224B-3 well (Figure 1, Table 1), a Sunniland test. A monocline on the Jurassic-Paleozoic contact, 10 km from the east end of this line, has expression through the entire overlying Mesozoic section (Fig. 23). Terminations and dip changes below the Jurassic-Paleozoic surface indicate extensive faulting in the Paleozoic section. The Texaco 2523 well lies at the juncture of lines 16 and 17. This well appears to be located on an eroded, Paleozoic high with a relief of 200 m. The eastern flank of this high may be controlled by a down-to-the east fault in the Paleozoic section (Fig. 23).

The salient feature of Line 16 (Figs. 22, 24) is a synclinal configuration of reflections within the Paleozoic rocks. The breadth of this feature, on Line 16, is at least 50 km; apparent relief on individual reflections is as much as two sec or approximately 6 km. Fig. 24 is an expanded view of the eastern flank of this syncline. The Texaco 2523 well appears to penetrate the angular unconformity between the westward dipping eastern flank of the Paleozoic Syncline and overlying Mesozoic sedimentary rocks (Figs. 22, 24). Relief of the high beneath Texaco 2523 appears to be related to erosion and has an apparent expanse of about 20 km. Horizontal multiple reflections overprint the dipping primary reflections that reveal the Paleozoic syncline. The intensity and continuity of these recognizable multiples serve as a warning that they probably are present elsewhere. Such multiples are very difficult to recognize where dipping primary reflections are lacking. Reflections on Line 16 above and including the Paleozoic-Jurassic contact are planar and dip very gently to the westsouthwest (Fig. 22). The Texaco well bottoms in over 300 m of rhyolite porphory cut by Jurassic diabase. A more resistant character of these volcanic igneous rocks may be responsible for the erosional high on the Paleozoic surface beneath the Texaco well. The volcanics probably consist of a sheet of rhyolite flows cut by diabase dikes. Together these igneous rocks may veneer underlying Paleozoic sediments.

Line 16 (Fig. 22) ends at the Mobil 3344 well. This well bottoms at 15782 ft. below sealevel in the uppermost Cotton Valley Formation of Late Jurassic age.

Line 15 (Figs. 1, 22) continues westsouthwestward from the Mobil 3344 well, 125 km, across the West Florida Escarpment. Dips in the Mesozoic sedimentary section, above and including the top Jurassic Cotton Valley Formation, are essentially flat. As a result of the westward deepening of the

shelf floor, the increased travel time duration in the water column enhances the appearance of the gentle westward dip in the shallow section. The Jurassic section shows marked onlap and thinning between the escarpment edge and a major, up toward the east, basement monocline 85 km east of the edge. Updip from the basement monocline, the rate of thinning and onlap to the Mobil 3344 well is almost imperceptible. It seems possible that the basement monocline marks a boundary at the updip limit of the Tampa Basin's south flank.

If our correlations and time-depth conversions are correct, it appears the Lower Trinity strata may crop out on the lower face of the escarpment on this profile. This is consistent with the Early Aptian age determinations on samples recovered aboard R/V ALVIN from the base of the escarpment at a depth of 10,716 feet (3266 m) reported by Paull (1986). D.C. Twichell (oral communication, 1988) attributes the terraces, that continue along strike on the lower part of the escarpment, to affects of differential erosion and corrosion of lithology variations in the platform edge. In light of the fact that the Trinity section typically consists of alternating carbonates and anhydrites, Twitchell's hypothesis seems very reasonable. The occurrence of anhydrite in the escarpment face near its base is also consistent with the observed sulfides in saline brines seeping at the escarpment base (Paull and Neumann, 1987).

A measure of the distorting effects of velocity contrast across steep carbonate escarpments is given by the fact that the Jurassic-Cretaceous event that appears to impinge on a terrace at 2850 m below sea level actually converts in depth to 6 to 7 km below sea level. This is essentially twice the depth of the basin floor.

The prograding sequence of reflections in the Cenozoic section is another point of interest regarding Line 15 (Fig. 22). This sequence begins at a point 10 km updip from the position of the basement monocline. The sea floor gradient steepens at this point. The sequence builds seaward, to the west, and ends at a deep shelf-edge, slope break that is accompanied by a second and even greater increase in the seafloor gradient. A lens of translucent sediment, 200 m thick, appears to infill against the upper slope of the prograded shelf edge. The dip on the surface of this lens parallels the dip of the underlying lower slope beds of the prograding sequence. The lower slope reflections of the prograding sequence pinch out some ten km from the platform-edge escarpment. The upper Cretaceous reflections are truncated seaward of this point and overlain by the translucent lens. The Upper Cretaceous section appears to have been totally eroded at the escarpment, so that the translucent lens directly overlies the Lower Cretaceous, shallow-water platform edge. Mullins and others (1987) contains admirably figured high-resolution reflection records showing the details of the internal structure of the Cenozoic seismic sequences in the outer Florida Shelf in this region.

The Sarasota Arch

Lines I, II, and III (Figs. 1, 25) comprise a strike profile across the boundary between the Sarasota Arch on the south and the Tampa Basin. Unfortunately these lines are of very poor quality. Line 1 extends 72 km from the Tenneco 3917 well on the south to the Shell 3912 well. This line reveals

essentially flat reflections with a few small offsets that may indicate faulting with throws of as much as 200 m at around 2 sec reflection time. A change in character marks an abrupt increase in background noise in the records at 2 sec. This time corresponds to a depth of about 4 km. Both the Tennaco and Shell wells encountered granitic basement rocks at depth of approximately 3.4 km so the increase in background noise may represent something other than variations in inpedance contrasts related to basement contacts.

Line II extends 52 km from the Shell 3912 well to the Mobil 3341 well on the north. This line's reflections show considerable dip change and terminations below 1 sec, probably related to faulting. There is, however, no correlation of events across terminations in the seismic data and it is thus impossible to determine the direction or amount of throw. Based on the well data, a sizeable down-to-the-north fault could be present between these wells. The Shell 3912 well encountered a contact between Early Commanchean or late Neocomian sediments and Paleozoic granites at 3444m subsea level. The Mobil 3344 well encountered the Cretaceous-Jurassic boundary at between 4097 m and 4505 m, penetrated about 1130 m of Jurassic sedimentary rock, and encountered either granite wash or granite volcanics between 5225 and 5460 m, depending on whether one accepts Mineral Management Service or operater picks on this well. Despite this disparity in picks in the Mobil 3341 well, it is clear that at least 5000 ft of Mesozoic section is present in the Mobil well that is missing in the Shell well. This missing section can be explained in a number of ways including nondeposition on a pre-Mesozoic basement high or uplift and erosion related to Mesozoic down-to-the-north faulting.

Line III extends northward, 38 km, from the Mobil 3341 well to the Mobil 3344 well. This line reveals numerous dip changes and terminations that appear to be related to faulting. Some of these inferred faults appear as shallow as 0.6 sec reflection time. Most faulting is down-to-the-north. Throws are 100 m or so. Multiples are a problem on all these lines.

Line IV (Figs. 1, 26) is a 290 km long eastnortheast to westsouthwest dip line extending from some 21 km seaward of the Calco Florida State 224 B-1 well, through the Tennaco 3917 well and eventually crossing the platform edge escarpment. The inshore 100 km of this line (SP 0-4000, Fig. 26) shows essentially planar reflections in the upper 1 sec that have some terminations and dip changes that may reflect karst pits, small scale faults, with throws of 10s of meters, or both. There is little or no expression of a structural high on our lines crossing the Tennaco 3917 well near S.P. 3750 (Fig. 1). The same applies to the second hundred kilometers of line although terminations and sags of reflections are somewhat more numerous and the seafloor depth begins to deepen noticeably toward the west. The succeeding 55 km of profile carries to the platform-edge escarpment. A down-to-the-west seafloor offset of 30 m or so at S.P. 8700 is accompanied by a marked increase in the westward seafloor gradiant. Four more seafloor offsets occur beyond this slope break, over the next 20 km of profile. Prograding Neogene foresets are apparent in the upper second of subbottom reflections beneath the easternmost 10 km of this line segment. Two slope breaks occur in the foresets beneath the two eastern seafloor offsets. The offsets may be related to shallow faulting resulting from downdip-thickening in shallow sections atop buried foreset slope breaks. Multiples make it difficult to determine whether faulting is present at the eastern offset points. Small-scale down-to-the-west faulting

does appear to be related to the sea floor offsets toward the west. The top of the platform edge escarpment occurs at S.P. 10250 (Fig. 26).

The West Florida Escarpment and Deep Gulf Basin

Line V (Figs. 1, 27) extends 230 km from southsoutheast to northnorthwest and ties the basinward ends of lines IV and VI (Fig. 1). This long, deep, basin strike line reveals planar continuous reflections stemming from impedence contrasts in the deep basin fill. The deepest correlatible event occurs at about 2.05 seconds subbottom at the junction of lines IV and V (Figs. 1, 27). It is clear from the downdip extremity of line IV (Fig. 26) that the event stems from an impedance contrast associated with a major unconformity, the so-called middle Cretaceous unconformity [MCU] of Buffler and others (1980), Freeman-Lynde (1983) and Buffler and others (1984).

The character of Line V (Figs. 1, 27) extends more or less unchanged, with a flat MCU, at about 6.5 sec, from the south end of the line to its midpoint. North of the midpoint, the MCU climbs from 6.5 to 6.3 sec over a 25 km distance and begins to show local positive relief related to underlying inferred salt swells in the northernmost 75 km of the line (Fig. 27). Events above MCU are essentially flat and continuous. Below MCU, terminations and dip changes indicate some faulting. Two broad inferred salt swells are particularly obvious in the northernmost 25 km of the line (Figs. 1, 28). The apparent widths of these features are 7 to 8 km and relief on MCU over these features is in excess of 100 m.

On Line IV, the MCU cuts down to a deep buried step (Fig. 29) whose top surface comes in at 1.8 sec sub-bottom and whose face slope lies some 20 km seaward of the exposed base of the escarpment. A number of overlying reflection packages, apparently bounded by unconformities, onlap and butt out on the buried lower slope of the platform-edge escarpment. This composite surface includes the basinward unconformity, the top of the buried step, the buried toe and slope of the platform-edge escarpment and the exposed escarpment slope. This surface carries upward and merges with the Early Cretaceous shallow-water platform edge and its apparent updip continuation that has also been referred to as the MCU in the platform interior setting (Massingill and Wells, 1987). This surface, of course, transgresses a considerable span of geologic time. Where it is exposed, the unconformity is Recent; and successively younger expanses of the buried escarpment slope and step surface have existed as erosion surfaces thoughout the Upper Cretaceous and Cenozoic . It follows that, in a strict sense, it is wrong to refer to this entire surface as a middle Cretaceous unconformity.

The expanse of Line IV extending 40 km from the escarpment east to the slope break includes a zone of relatively steeply dipping sea floor (the apparent gradient is approximately 40 m/km) (Fig. 29). At the seaward edge of this zone, a 10-km-broad expanse of gently eastward dipping reflections lies immediatly east of the escarpment edge. These dips are to some extent subdued by the east-to-west water depth gradient overlying them. The dips indicate that the uppermost Lower Cretaceous platform edge was slightly elevated over the adjacent platform interior during the time span represented by the 2 km thickness of platform-edge history visible above the multiples on line IV. From the allignment of diffractions of the platform edge, the apparent dip of

the feature is about 45°. The actual dip is slightly steeper because line IV varies about 10° from a true dip crossing of the platform edge.

The horizontally squeezed section of the escarpment crossing in line IV (Fig. 29) accentuates the sea floor offsets and slope breaks of the outer deeper platform margin and makes obvious the relationship of these features to down-to-the-basin normal faults at the platform edge. The nature of the anticlinal step of incoherant reflections visible just downdip from the buried toe of the escarpment slope is unknown. This feature may be either a carbonate pinnacle or salt swell.

The platform edge crossing on line VI (Figs. 1, 20, 30) lacks the precipitous relief seen on many such features. The apparent slope angle is 8.5°. The line is approximately 20° off perpendicular to the strike of slope so the true slope angle is about 10°. The junction of the outer platform margin and platform-edge slope occurs at SP 1850 (Figs. 1, 30) at a depth of 1500 m. The base of the exposed slope is at a depth of 3225 m so the relief of the slope is 1725 m. The zone of incoherent reflections inferred to be shallow-water, platform-edge facies underlies the edge of the platform and has an apparent lateral expanse of 4 km at its crest. Slight dip changes in the seaward margin of the platform interior facies indicate a down-to-the-basin, normal fault with a throw of 100 m. Dips in the platform interior facies, where they abut the platform edge facies, indicate that the edge facies had a positive relief of about 100 m over the adjacent interior. The platformward continuation of the unconformity capping the edge facies is overlain by a thin translucent interval, 100 to 200 m thick, of Upper Cretaceous to Early Paleogene chalky facies. This unit is capped by a unit containing numerous unconformities that probably represents both Paleogene and Early Neogene sediments. The unconformitites truncate the Upper Cretaceous and Early Paleogene unit at the platform edge. The uppermost truncation surface cuts out the entire zone of Early Neogene through the Upper Cretaceous so that a 200 m thick unit of translucent Upper Neogene sediments containing some low-angle reflections suggesting prograding foresets, overlies the Lower Cretaceous edge facies. The foreset unit pinches out downslope about 2 km from the Lower Cretaceous crest in a water depth of 2250 m. The interval of Paleogene to Early Neogene unconformities contains a number of hummocky reflections. The hummocks are up to 2 km long with reliefs approaching 100 m and are suggestive of some sort of incised waveform superimposed on muddy pelagic carbonate chalks by activity of bottom currents.

The platform edge slope is rough, as evidenced by the large number of diffractions obscuring its surface. Seaward of the exposed slope, the reflection band marking its surface merges with the mid-Cretaceous unconformity. The unconformity is clearly onlapped by overlying younger sediments characterized by horizontal continuous reflections. Folds, in the section beneath the unconformity are as broad as 5 km with reliefs of a few 100 m and may be related to salt swells. A possible diapir rises to the unconformity at SP 850 (Fig. 31).

Line 15 (Figs. 1, 31) offers our best control on the relationship of platform stratigraphy to the platform edge escarpment. The line extends 145 km westsouthwestward from the Mobil 3344 well to the platform edge escarpment and continues another 15 km over the deep Gulf Basin beyond the platform edge. The Mobil 3344 well bottoms at 4810 m in oldest Cretaceous or

youngest Jurassic beds. The corresponding reflection band carries seaward almost to the escarpment, where its appearance in a time section is more or less at the level of the adjacent basin floor. Time-depth conversion establishes the position of this reflection band at 6 to 7 km below sea level, essentially twice the basin depth. The severity of the velocity pull-up of reflections in the platform block make it extremely difficult to match reflections within the block to bottom topographic features such as terrace surfaces on the platform escarpment. It is possible to carry a Paleozoic-Mesozoic reflection, B (Fig. 31), based on an updip tie at the Texaco 2523 well (Figs. 1, 22), across the extent of line 15. This reflection appears to be overlain by at least 2.5 km of inferred Late Jurassic sedimentary rock at the platform edge. The Jurassic wedge thins eastward, onlapping the Mesozoic-Paleozoic contact, to an apparent thickness of 800 m at the Mobil 3344 well. Approximately 400 m of the Jurassic thinning occurs on a basement monocline between SP 1000 and 800 (Figure 22). Reflections in the Late Jurassic to Lower Cretaceous interval are continuous and relatively planar, with thinning of less than 10 percent from the platform edge to the Mobil·3344 well. The Upper Cretaceous to Paleogene interval varies in thickness in response to apparent erosion at its top and appears to be almost totally cut out at the platform edge. The Cenozoic interval in dominated by reflections whose foreset geometry indicates progradation from the east. An inferred Neogene slope edge occurs 25 km east of the platform edge and is associated with a perceptable sea-floor slope break. Seaward of this Neogene edge, the uppermost reflection bounding the slope front fill merges downdip with an apparent erosion surface that truncated much of the Upper Cretaceous interval at the platform edge. Between the escarpment and the Neogene edge, a translucent blanket of latest Cenozoic sediment, approximately 300 m thick, infills the Neogene slope relief and continues to the platform edge.

The relief of the platform edge above the adjacent basin floor, at 3300 m, is about 1600 m. Between the crest of the terrace, at 2850 m and the crest of the escarpment at 1650 m, the allignment of diffractions off the slope indicates an average angle of declivity of at least 45°. Seaward of the base of the exposed escarpment slope, the reflection marking the mid-Cretaceous unconformity rises from 0.9 sec subbottom to merge with the sea floor at the base of the lower escarpment step. Overlying basinal section clearly onlaps the unconformity.

SUMMARY AND CONCLUSIONS

This interpretation of our seismic reflection data forces a number of constraints on our initial working hypothesis regarding the nature of the crust beneath the Western Florida Shelf. Rather than blocks of Pre-Mesozoic continental crust separated by zones of extension or spreading underlain by extensively rifted, transitional, or Jurassic, oceanic crust (Klitgord and others, 1984), the seismic and well data available to us indicate a vast expanse of Paleozoic rock that essentially underlies the entire platform north of 26°N. Highs and lows (arches and basins) within this region do exist, but both positive and negative areas appear to be underlain by substantial thicknesses of predominately sedimentary or metasedimentary Paleozoic rocks. It follows that if any oceanic crust is present in the foundation of the Western Florida Shelf, it must be Paleozoic or older in age and must lie below the depth of penetration of our 8-second records.

Rift-style faulting of pre-Jurassic rocks is commonest in the Apalachicola Basin and northern port of the Middle ground Arch (Figs. 3, 4, 6-12, 16, 17). This style of faulting, consisting of half graben formation, is not restricted to basinal settings; nor to Late Triassic-Early Jurassic age of formation. One of the best examples seen on our records occurs on line VII (Fig. 16) where the graben fill appears to be Paleozoic in age. However, enough of the fault activity is identified as Late Triassic to Early Jurassic to justify the inferrence that this region was involved in the initiation of the Atlantic-Gulf sea-floor spreading event.

The density of our data is insufficient to map fault patterns. However, on the Destin Dome's northern and eastern flanks (Figs. 7, 8, 9, 11, 12), a system of deep faults, primarily active in Late Jurassic time, appears to bound the region of thick Jurassic salt that forms the pillow responsible for the Destin structure. A major, down-to-the-west fault (Figs. 3, 6) forms the eastern limit of the thicker salt region and is inferred to continue northwestward into the onshore Pickens-Pollard fault trend. Antithetic, northward dipping faults, compensating this major fault, bound the Destin Dome's north flank (Figs. 7, 8, 9, 11). Although the major throw on these faults occurred during Late Jurassic, they continue upward into beds of Neocomian age. Flowage of the salt is responsible for the best defined structures seen in the study area: Pillows with planar floors and relatively gently arched roofs are visible at the Gulf 2468 structure (Figs. 3, 4), the Destin Dome (Figs. 3, 5-9, 11) and south of Destin Dome (Figs. 7, 10). The Gulf structure and the structure downdip from Destin Dome have relatively early growth histories that appear to have commenced in the Jurassic and continued into the Neocomian. At Destin Dome, the structure appears to have begun forming in Late Early Cretaceous and continued into the Cenozoic. Erosion and infilling of local lows at the top of the salt interval at Destin Dome (Fig. 5) may cause thickness variations in the Norphlet Formation, an attractive potential reservoir section that overlies the salt. A shallow crustal faulting pattern on Destin Dome (Figs. 7-9, 11) probably is a result of upward arching attended by extension. These faults may provide escape routes for fluids from deeper permeable sections of the dome.

South and west of the deep Destin fault system, separate reflection bands (reflections S and B of figures 3-11) are related to the top and base salt seismic impedance contrasts. East of the fault system, these reflection bands

merge, implying a pinch out or substantial thinning of the salt interval. The merged reflection (B, for "basement") stems from velocity and density contrasts at the Paleozoic-Mesozoic contact. The intensity of this reflection band weakens toward the south, as the seismic impedance of relatively salt-free Mesozoic section increases, to more nearly match that of the underlying Paleozoic rocks.

Confusion can arise from the accepted convention of referring to the top of the Paleozoic section as the "basement" boundary. This practice probably gained acceptance because points of control on the crystalline basement over much of the Florida region are few or nonexistent and because the Mesozoic-Paleozoic contact is the seismic basement in the sense that it is related to the deepest correlatable reflection that can be mapped over much of the Florida region. In principle, a preferrable alternative was followed by Klitgord and others (1984). They referred to this surface as the pre-Cretaceous, postrift unconformity surface. The surface is a seismically impressive, complex and compound unconformity. The problems in their terminology arise from the facts that the surface is overlain by inferred rift-phase salt of supposed Callovian age and onlapped by the Norphlet, Smackover, Haynesville, and Cotton Valley formations, of Late Jurassic age, and the entire Early Cretaceous section. On the Peninsular Arch, the surface is capped by Late Cretaceous rocks. It follows that parts of this surface are at least older than the rift-phase salt and at least as young as mid-Cretaceous. Thus the adjectives post-rift and pre-Cretaceous are not strictly applicable, to this surface. When we refer to this surface as "basement" we do so with the proviso that it is seismic basement we're talking about.

Glimpses of structures within and on top of the Paleozoic section are visible at various points in our records. Monoclines (Figs. 13, 22, 23) that appear to be primarily related to intrabasement faulting occur at a number of locations identified by Klitgord and others (1984) as hinges and fracture zones. These zones do appear to be fault-related and the faulting and thickness variations carry upward, in some cases, into the lower Mesozoic section. This supports the trend of faults in the foundation of the Florida Platform, more or less conforming to the pattern of fracture zones inferred by Klitford and others (1984). The "hinge zones" however are not boundaries of isolated continental blocks envisioned by these authors (Klitgord and others, 1984). Zones of rough diffracting basement surface (Figs. 12, 14, 15) may result from faulting or differentially eroded intrusives at the Mesozoic-Paleozoic contact. Intermittent expanses of high amplitude "basement" reflections (Figs. 12, 14, 15) may result from presence of patches of extrusive igneous rocks on the Paleozoic surface.

A sizeable intrusion may be the source of the major intrabasement high approximately 13 km beneath the northeastern end of line 12 (Figs. 18 and 19). Only the western flank of this feature is visible in our data but it does appear to have associated faulting in the overlying Paleozoic and Mesozoic section so that its emplacement may be Mesozoic in age. This feature appears to agree in position with a major gravity minimum figured by Klitgord and others (1984). This correlation favors an acidic composition for this inferred intrusive body.

Although unrevealed by our seismic data, a major fault, down-to-the-north, with 5000 ft of throw, is indicated by examination of the downthrown

Mobil 3341 well and the upthrown Shell 3912 well (Fig. 1) and may mark the boundary between the Sarasota Arch and Tampa Basin or southeastern extension of the Middle Ground Arch (Fig. 2).

From our analysis, it is apparent that there is considerable lack of balance in the definition and distinction of the various basins and arches that form the subelements of Western Florida Shelf. The Apalachicola Basin (Fig. 2), if defined as the zone of thick Jurassic salt confined by the deep, Late Jurassic, fault system north and east of Destin Dome, appears to be a reasonably well defined tectonic element of the Western Florida Shelf. This basin may be thought of as a Jurassic basin in that it contains a thickened salient of Jurassic salt, but not in the sense that it is underlain by Jurassic oceanic crust.

The Middle Ground Arch (Fig. 2) on the other hand, is poorly defined on our data. This broad, low-relief arch appears to be a westward projecting nose that is onlapped from the north and west by rocks as old as Late Jurassic. Erosional peneplanation appears to have shaped this arch that is traceable onshore into the west flank of the Peninsular Arch. Erosion on the continually decreasing area of exposed Paleozoic rocks continued into the middle Cretaceous and ended with the burial of the last exposure zone on the crest of the Peninsular Arch. The basement ramp extending from the offshore Middle Ground Arch to the onshore Peninsular Arch includes portions of the East Sawanee Basin (Fig. 2). The basinal character of that tectonic feature is a function of the accumulation of Paleozoic sediments in the area prior to the uplift and erosion that formed the Peninsular Arch and its poorly defined offshore adjunct. Although faults and intrusion of Pre-Cretaceous Mesozoic age appear to cross the Middle Ground Arch from southeast to northwest, there is no evidence in our data substantial strike-slip motion on these faults.

The Tampa Basin is another equally elusive tectonic element. A monocline seen on line 15 (Fig. 22) may represent a point on the northeastern boundary of this basin with the adjacent Middleground Arch. A point of control on the Tampa Basin's or Middleground Arches' southeastern boundary against the Sarasota Arch (Fig. 2) is inferred from the expansion of section seen in the Mobil 3341 well relative to section in the Shell 3412 well (Fig. 1). Although the Sarasota Arch is invisible in our seismic coverage, its existance has been firmly established by drilling (Shell 3912 well, Odeco 3909 well, Tenneco 3417 well and Mobil 3903 well, Fig. 1, Table 1). The limits of this arch have not yet been established; however, the 5000-ft relief on its northwestern flank indicates that it rivals the Peninsular Arch in structural significance.

References

Addy, S. K. and Worzel, J. L. 1979. Gas Seeps and Subsurface Structure off Panama City, Florida: American Association Petroleum Geologists; v. 63, p. 668-675.

Addy, S. K. and Buffler, R. T. 1984, Seismic Stratigraphy of the Shelf and Slope. Northeastern Gulf of Mexico: American Association Petroleum Geologists Bulletin, v. 68, p. 1782-1789.

Applegate, A. V. and Lloyd, J. M., 1985, Summary of Florida Petroleum Production and Exploration, Onshore and Offshore through 1984: Florida Geological Survey, Information Circular No. 101, p. 1-69.

Ball, M. M., Martin, R. G. and Taylor, D. 1982, Destin Dome and Western Florida Shelf (abs): American Association Petroleum Bulletin; v. 66, p. 544-545.

Buffler, R. T., Watkins, J. S., Shaub, F. J. and Worzel, J. L. 1980, Structure and Early Geologic History of the Deep Central Gulf of Mexico Basin, in Proceedings of a Symposium: The Origin of the Gulf of Mexico (Pilger, R. H.; Editor); Baton Rouge, Louisiana, Louisiana State University. p. 3-16.

Buffler, R. T., Schlager, W., Bowdler, J. L., Cotillon, P. H., Halley, R. B., Kinoshita, H., Magoon, L. B., III, McNulty, C. L., Patton, J. W., Silva, I. P., Suarez, O. A., Testarmata, M. M., Tyson, R. V., and Watkins, D. K., 1984, Initial reports of the deep-sea drilling project: v. LXXVII: Washington, D.C., U.S. Government Printing Office, 747 p.

Freeman-Lynde, R. P. 1983, Cretaceous and Tertiary Samples Dredge from the Florida Escarpment, Eastern Gulf of Mexico: Trans. Gulf Coast Association Geological Societies, v. 33, p. 91-99.

Gee, W. L., Hill, D. S., Oakes, R. L., Pert, D. M. and Reed, J. C. 1976, Texaco No. 1, OCS-G2516 Apalachicola South Area, Block N659-E158: Geological and Operational Summary: U.S. Geological Survey, Conservation Division, p. 1-49.

Klitgord, K. D., Popenoe, P. and Schouten, H., 1984, Florida: A Jurassic tranform plate boundary: Journal of Geophysical Research, v. 89, p. 7753-7772.

Lloyd, J. M., 1985, Annotated Bibliography of Florida Basement Geology and Related Tectonic Studies: Florida Geological Survey, Information Circular No. 98, p. 1-72.

Martin, R.G., 1975, Bathymetric Chart of the Gulf of Mexico Region 1:2,500,000: U.S. Geological Survey Open File Map 75-140.

Massingill, L. M. and Wells, R. H., 1987, Maps Showing Distribution of the Middle Cretaceous Unconformity in the Eastern Gulf of Mexico: U.S. Geological Survey Miscellaneous Field Studies Map, MF-1984.

Mullins, H. T., Gardulski, A. F., Wise, S. W., and Applegate, J., 1987, Middle Miocene oceanographic event in the eastern Gulf of Mexico: Implications for seismic stratigraphic succession and Loop Current/Gulf Stream circulation: Geological Society of America Bulletin, v. 98, p. 702-713.

Paull, C. K., 1986, I. Florida Escarpment: Chemosynthetic Communities, Geochemical Processes and Geologic Consequences. II. Stable Isotope Signal Carriers in Fine Pelagic Carbonates: San Diego,University of California, Ph.D. thesis 196 p.

Paull, C. K., and Neumann, A. C., 1987, Continental Margin Brine Seeps: Their Geologic Consequences: Geology, v. 15, p. 545-548.

Figure Captions

Figure 1. Index Map. Bottom contours in meters. 32-fold seismic coverage obtained with 3200 m streamer and 2000 in^3 airgun-array source indicated by thick lines, numbered with arabic numerals, with cross hatches at 200 shot point (SP) intervals and arabic numerals indicating shot points at 5000 SP intervals in thousands. 24-fold seismic coverage obtained with a 1200 m streamer and 550 in^3 airgun source indicated by thin lines, numbered in roman numerals, with cross hatches at 1000 SP intervals and arabic numbers indicating shot points in thousands at 5000 SP intervals. Well letter designations are as follows: Gulf 2468; Exxon 2486; Amoco 2502; Sun 2490; Cal 224-A2: California Co., Florida State 224A-2; Texaco 2516; Cr-1: Coastal Petroleum, Ragland-1; Shell 2527; Texaco 2523; Cal 224-B3: California Co., Florida State 224 B-3; Mobil 3344; Mobil 3341; Shell 3912; Mobil 3903; Odeco 3909; Tennaco 3917; Cal 224-B1: California Co., Florida State 224 B-1; Mobil 224-B1: Mobil, Florida State 224 B-1.

Figure 2. Schematic tectonic map of the Florida-Bahamas-Cuba Region (from Klitgord and others, 1984). Predominant magnetic anomaly lineations are indicated: East Coast magnetic anomaly (ECMA), Brunswick magnetic anomaly (BMA). Blake Spur magnetic anomaly (BSMA). Basement hinge zones (hachured) separate inferred Jurassic marginal basins from Paleozoic and older crust. Only the most important fracture zones (FZ) are shown. Bathymetric contours (from Martin, 1975) are shown in meters.

Figure 3. Regional strike profile of Apalachicola Basin composed of Lines 1, 2, 3 and the western end of Line 8 (Fig. 1). The profile extends 250 km from the Gulf 2468 well on the west, across Destin Dome, through the Exxon 2486 well, through the Sun 2490 well, and continues for 1700 SP (56 mi, 85 km) past the Sun well to its eastern end on the northwestern flank of the Middle Ground Arch. Salient features of this line are the Gulf 2468 structure's crest and eastern flank (a); the Destin Dome, west flank (b'), crest (b''), and east flank (b'''); the down-to-the-west major fault (c), marking the boundary between the Apalachicola Basin and the Middle Ground Arch. Letters in margin indicate inferred stratigraphy of specific reflection bands: B denotes Jurassic-preJurassic contact referred to as basement; S denotes basal Jurassic sediment on salt or basement; CV is top Cotton Valley; H is top Hosston; K_L is top Lower Cretaceous; The S and B reflection bands merge east of the major fault (c) as the salt interval pinches out. A depositional anticline associated with thickening in the Cotton Valley (CV) to Hosston (H) interval and persisting as a draped anticline through Cretaceous to Paleogene time, occurs at (d). A wedge-out of onlapping upper Comanchean section on a major intra-Comanchean unconformity that may be associated with the Ferry Lake - Punta Gorda Anhydrite of Trinity (early Comanchean) age is indicated at (e). Locations of figures 4-6 are indicated at the base of appropriate panels of this regional strike profile.

Figure 4. Gulf 2468 structure, eastern flank. Reflections in the pre-Cretaceous appear to onlap this structure's eastern flank (a). There is slight thinning in the latest Jurassic, Cotton Valley (CV) interval and in the oldest Cretaceous, Hosston (H) interval. Closure on this structure ceases at the top of the Lower Cretaceous section (K_L). The basement reflection (B) is slightly depressed beneath this structure (b). Dip changes and diffractions indicate possible faults (c). Intrabasement reflections dip toward the west (d) and are truncated by the reflection at the basement surface.

Figure 5. Expanded record section on the crest of Destin Dome. Lensoid configurations of reflection packages infilling lows occur near the salt-sediment contact (a). Terminations and dip changes indicating possible faulting occur at the basement surface and continue upward into the Jurassic interval (b). Shallow faulting is present just west of the Sun 2490 well (c).

Figure 6. Major fault 8 km east of the Sun 2490 well. Throw on the fault (a) is at least 1000 m on the top salt-base Jurassic sediment reflection (S) and the fault as evidenced by terminations that continue upward (b) through the lowest Cretaceous, Hosston interval (H).

Figure 7. Destin Dome dip lines. Thinning (a) indicative of growth history appears to span latest Early Cretaceous (post-Hosston) through Cenozoic time; S denotes the thick bend of reflections marking the top salt-base of Jurassic sedimentary rock interval (b). Late Jurassic through earliest Cretaceous faulting is indicated by diffractions and terminations (c) bordering the Destin Dome's north flank. Terminations and offsets (d) indicate small, post Hosston (H) faulting apparently related to downdropping of the dome's crest. Some of the faults appear to cut nearly to the seafloor.

Figure 8. Expanded section of line 4 over the Destin Dome crest. The major, latest Jurassic to oldest Cretaceous fault (a) borders the structure's north flank. Shallow faulting (b) is limited to the structural crest.

Figure 9. Expanded section of line 5 over the Destin Dome crest. A well defined diffraction (a) marks the faulted boundary of the Late Jurassic sediments - salt reflection band. A profusion of relatively late shallow faults (b) is concentrated on the crest of the dome.

Figure 10. Expanded section of southern end of line 6-7. A Jurassic-Early Cretaceous high (a) overlies a flat base salt-basement reflection (b). Reflections from lowest Jurassic sedimentary rocks appear to pinch out on the northern flank (c) of the inferred salt swell. Southward dipping intrabasement reflections (d) are visible below the salt-basement reflection.

Figure 11. Expanded section of the northern part of line 6-7. Shallow faulting on the dome's crest (a) is revealed by terminations with slight offsets (throws of 10 s of meters) above the Hosston (H) reflection band. The Late Jurassic to earliest Cretaceous fault off the north flank of the dome (b) is revealed by diffractions at the sediment-salt reflection band (S). This fault offsets reflections up to at least the top of the Hosston (Neocomian) interval (H).

Figure 12. Regional strike profile of line 8, across the western flank of Middle Ground Arch. The northwestern limit of arch is taken as the Late Jurassic - Early Cretaceous fault east of the Sun 2490 well (a). Eastward from this fault, the seismic definition of the salt interval disappears and the top salt-base sediment reflection appears to merge with the salt-basement reflection. A basement monocline (b) occurs at the point at which the seismic impedence contrast between Late Jurassic sedimentary rocks and Paleozoic "basement" rocks ceases to give rise to a well defined "top basement" reflection. Sporadic disappearance of this reflection (c) occurs for short (5 km or less) intervals west of the monocline. The last prominent reflection marking the Jurassic-Paleozoic basement contact (d) occurs 30 km farther southeastward along line 8. Over the remaining 100 km of profile climbing the flank of the arch to its crest at the Texaco 2516 well (e), the most prominent reflection is associated with the Neocomian-Commanchean contact at the top of the Hosston interval (H).

Figure 13. Basement monocline (a) on line 8. A zone of broken reflections (b) is inferred to be related to basement topography. The Jurassic-Paleozoic basement reflection band dies out southeast of this monoclinal structure.

Figure 14. Zone of broken Jurassic-Paleozoic basement reflection band (a) on line 8. Zones bordering strong basement reflection appear to have positive relief of approximately 100 m and are apparently fault bounded with diffractions at their margins.

Figure 15. Southeastward continuation of the strike line across Middle Ground Arch continuing from the Texaco 2516 well down the southeastern flank of Middle Ground Arch along seismic lines 13 and 14. The Shell 2527 well occurs at the junction of lines 13 and 14 (Fig. 1). No expression of updip extension of the Tampa Basin (Fig. 2) is visible on lines 13 and 14. A strong reflection band marking the Jurassic-Paleozoic basement contact is lacking over most of the strike coverage on lines 13 and 14. Patches of reflection (a) at this contact occur that are similar to the short segments of high-intensity reflection on the northwestern flank of the Middle Ground Arch (Figs. 12, 14).

Figure 16. Updip strike line extending northwest to southeast across the Middle Ground Arch along line VII (Fig. 1). A basement graben can be seen at (a). The basement reflection is marked at (B). Intrabasement reflections appear to onlap the lower graben fill toward the west (b). Thus it appears that this graben may have

formed during Paleozoic time. This figure has been squeezed to accentuate low angle dips. Vertical exaggeration at the "basement" surface is about 4X.

Figure 17. Northeastern dip line on the Middle Ground Arch including seismic lines 9 and 10 (Fig. 1). The Cal 224-A2 well lies 3.2 km northwest of the northeast end of this line. A band of high intensity reflections (B) probably marks the contact of a diabase sill with underlying Eagle Mills red beds (Triassic) encountered in the Cal 224-A2 well. The southwestern terminus of this reflection band (a) occurs 35 km from the Cal 224-A2 well. The reflection band at (b) may represent a contact between Triassic graben-fill and underlying Paleozoic basement rocks. To the southwest of the reflection terminations inferred to be associated with the top and base of the graben fill, a high amplitude reflection band occurs at 2.4 sec (c). The strength of this reflection band varies. A particularly high intensity segment with slight northeast dip occurs at (d). A dip reversal is apparent on this reflection package at (e) at the intersection with line 8. Expression of this dip reversal vanishes above the reflection band near the top of the Hosston (Neocomian) interval (H). The band marked at (c) is the Jurassic-Paleozoic "basement" contact. A possible graben fill (f) occurs beneath the southeasternmost 15 km of line 10.

Figure 18. Axial dip line on the Middle Ground Arch along seismic lines 11 and 12 (Fig. 1). Lines 11 and 12 join at the Texaco 2516 well (Fig. 1, Table 1). The Coastal Ragland No. 1 well lies 40 km (25 mi) northeast of the northeast end of line 12. Both the Texaco 2516 and the Coastal Ragland No. 1 wells bottom in Paleozoic sedimentary rocks. The planar character of the reflection band marking the Jurassic-Paleozoic basement contact suggests peneplaination. Local relief probably reflects differential erosion and is responsible for drape structures in overlying Jurassic and Neocomian sedimentary rocks. A major intrabasment high (a) occurs beneath the northeastern end of line 12.

Figure 19. Expanded time section of the intrabasement high (a) occurring beneath the northeastern end of line 12 (Fig. 18). The 4.4 sec reflection time on the crest of this feature corresponds to a depth of approximately 13 km. This feature may represent an intrusive igneous body.

Figure 20. Southeastern dip line on the southeastern flank of the Middle Ground Arch along seismic line VI (Fig. 1). Multiples below 2 seconds obscure primary reflections on this profile. Cenozoic section is restricted to the upper second. A major portion of middle to lower Cenozoic section consists of reflections suggesting basinward progradation (a). The northeasternmost 2000 shot points on this line contained no useful data and are not included in this figure.

Figure 21. Expanded time section showing reflections suggesting basinward

progradation of middle and lower Cenozoic section on seismic line VI (see Figure 20 for location).

Figure 22. Regional dip line within the Tampa Embayment that separates the Middle Ground Arch and the Sarasota Arch. This dip line is composed of seismic lines 15, 16 and 17 (Fig. 1). The updip, eastnortheastern end of line 17 is 16 km southwest of the Cal 224-B3 well (Fig. 1, Table 1). A monocline (a) on the Jurassic-Paleozoic surface, 10 km from the east end of this line, has expression throughout the Mesozoic section. Terminations and dip changes below the Jurassic-Paleozoic reflection band indicate extensive faulting in the Paleozoic basement. Lines 17 and 16 join at the Texaco 2523 well (b). A synclinal configuration (c) of Paleozoic reflections is the main feature seen on line 16. Lines 16 and 15 join at the Mobil 3344 well. Line 15 continues west southwestward across the escarpment (g) at the western edge of the Florida shelf. The Jurassic section shows marked onlap and thinning between the escarpment edge and a monocline (d) on the Jurassic-Paleozoic basement reflection band 85 km east of the escarpment. Updip, between this monocline and the Mobil 3344 well (e), the rate of thinning and onlap in the Jurassic section is almost imperceptible. The basment monocline may represent the updip extent of the Tampa Basin. Note the prograding sequence of reflections (f) in the Cenozoic section.

Figure 23. Expanded time section of the monocline (a) on the Jurassic-Paleozoic "basment" contact with drape structure in the overlying Mesozoic and Cenozoic section. See Figure 22 for location.

Figure 24. Expanded time section showing the eastern half (a) of the synclinal configuration of intrabasement reflections beneath seismic line 16. See Figure 22 for the location of this figure.

Figure 25. Strike line across the Sarasota Arch into the Tampa Basin composed of seismic lines I, II and III (Fig. 1). All these lines are of poor quality with limited penetration and overprinting by multiples. Line I extends 72 km from the Tenneco 3917 well (a) to the Shell 3912 well (b). Reflections on line I are essentially flat with small offsets that may indicate faults with throws of less than 200 m at 2 sec reflection time. There is an abrupt increase in background noise, below 2 sec, at approximately 4 km depth on this line. Line II extends 52 km from the Shell 3912 well to the Mobil 3341 well (c). This line shows considerable dip variation and terminations below 1 sec that are probably related to faulting. There is no correlation of events across terminations so senses and amounts of fault throw are indeterminable. Based on the well data, a sizeable down-to-the-north fault could be present on line II. The Shell 3912 well encountered a contact of early Comachean or late Neocomian sedimentary rocks on Paleozoic granites at -3444 m. The Mobil 3341 well penetrated 1130 m of Jurassic sedimentary rocks over granitic volcanics or granite wash at -5225 to -5460 m. Thus, approximately 5000 ft of Mesozoic section in the Mobil 3341 well is missing in the Shell 3912 well. Line III extends 38 km from

the Mobil 3341 well to the Mobil 3344 well (d). Numerous dip changes and terminations indicate down-to-the-north faulting as shallow as 0.6 sec. Throws on these shallower faults are approximately 100 m.

Figure 26. Regional dip profile across the Sarasota Arch, line IV (Fig. 1). Line IV extends 290 km west southwestward from 21 km seaward of the Calco Fl. St. 224 B-1 well through the Tenneco 3917 well (a) and continuing across the platform edge to the deep Gulf basin at its western end. The inshore 100 km of this line shows terminations and dip changes in the upper 1 sec which reflect karst pits or small faults with throws of 10's of meters. Terminations and sags of reflection bands are more numerous in the second 100 km. A down-to-the-west seafloor offset at S.P. 8700 (b) is accompanied by an increased westward sea floor gradient. Four additional sea floor offsets occur between S.P. 8700 and the platform edge. Prograding foreset slope breaks underlie two of the seafloor offsets. The offsets may result from faulting associated with differential compaction in the thickened fill over the slope of the underlying progradational sequences.

Figure 27. Regional basinal strike line, Line V extends 230 km (144 mi), southsoutheast to northnorthwest, tying the basinward ends of Lines IV and VI in the deep Gulf basin. This line reveals planar, continuous reflections stemming from impedance contrasts in the deep basin fill. The deepest correlatible event seen on line V occurs at the junction with line IV (Fig. 26) at 2.05 sec subbottom. This event is identifiable as a major unconformity on line IV (Fig. 26). The unconformity has been referred to as a middle Cretaceous unconformity (MCU) (Buffler and others, 1980). Over the southern half of line V, MCU is essentially flat at 6.5 sec. North of the line's midpoint, MCU climbs to 6.3 sec and begins to show relief related to underlying salt swells (a). Events above MCU remain essentially flat. Below MCU, terminations and dip changes indicate some faulting.

Figure 28. Expanded time section across salt swells (a) encountered along the northern portion of line V (Fig. 1, 27). The apparent breadth of these swells is 7 to 8 km and relief on MCU over these features is more than 100 m.

Figure 29. Expanded time section of the platform edge crossing on line IV (Figs. 1, 26). MCU cuts down to a buried step (a) at 1.8 sec subbottom, 20 km seaward of the exposed base of the platform edge escarpment (b). A number of overlying reflection packages, bounded by unconformities, onlap and butt out against the buried lower slope of the platform edge (c). The composite reflection band marking the seaward extend of MCU, the top of the buried step, buried slope of the platform edge and exposed platform edge appears to continue upward into the reflection at the upper surface of the Early Cretaceous shallow water platform (d) continuing into the platform interior setting. This reflection band on the platform has also been referred to as the MCU. This reflection band transgresses a considerable span of geologic

time. The outer 10 to 15 km broad zone of the Lower Cretaceous platform edge appears to have been slightly elevated over the adjacent platform interior (e). Alignment of diffractions of the platform edge indicate the apparent dip of this feature is 45°. This squeezed section accentuates seafloor offsets and slope breaks (f) and makes obvious the relationship of these features to down-to-the-west faults in the platform margin (g). The anticlinal steps (a) downdip from the toe of the escarpment may be either carbonate buildups or salt swells.

Figure 30. Expanded time section of the platform edge crossing on line VI (Figs. 1, 20). This platform edge crossing lacks the precipitous slope seen to the south on line IV (Fig. 29). The slope angle on line VI is only 10°. Slope relief is 1725 m. The zone of incoherent reflections (a) marking the platform edge facies has an apparent width of 6 km. Dip change (b) at the northeast boundary of the edge facies indicate a possible down-to-the-west normal fault. The edge facies nevertheless appears to have positive relief of 100 m over the adjacent platform interior. Upper Cretaceous and Paleogene units appear to be truncated updip from the platform edge so that only a 200 m thick, seismically translucent unit (c), of inferred Neogene section appears to overlie the Lower Cretaceous rocks at the edge. Hummocky reflections (d) 2 km broad and 100 m high suggest a waveform incised by bottom currents in the muddy pelagic Cenozoic carbonate rocks. Seaward of the platform edge, the MCU reflection band rises to merge with exposed platform slope (e). Folds (f) in the section beneath the MCU are as broad as 5 km with reliefs of as much as 100 m and may be salt swells.

Figure 31. Expanded time section of the platform edge crossing on line 15 (Fig. 1, 22). Line 15 represents our best control on time stratigraphic relationships within the platform edge. This line extends 125 km westsouthwestward from the Mobil 3344 well to the platform edge escarpment. We have carried reflection ties from the base of the Mobil 3344 well into the platform edge. A measure of the tremendous effects of the velocity contrast across steep carbonate escarpments is given by the fact that the Top Neocomian event (H) that appears to impinge at (b) on a seafloor terrace at 2850 m actually converts in depth to 6 to 7 km below sealevel which is essentially twice the depth of the basin floor. The Paleozoic-Jurassic reflection (B) appears to be overlain by 2.5 km of Jurassic sedimentary rock beneath the platform escarpment. This Jurassic wedge thins eastward, onlapping the basement contact, to a thickness of only 800 m at the Mobil 3344 well. An erosion surface on the platform edge (d) truncates much of the Upper Cretaceous section. A translucent blanket of Neogene sediment (e), 300 m thick, overlies the unconformity and extends to the platform edge. This blanket abuts a slope break (f) on the east. Allignment of diffractions on the slope indicates an angle of declivity of 45°. The reflection marking the MCU rises from 0.9 sec subbottom to merge with the lower of two steps (g) on the exposed escarpment.

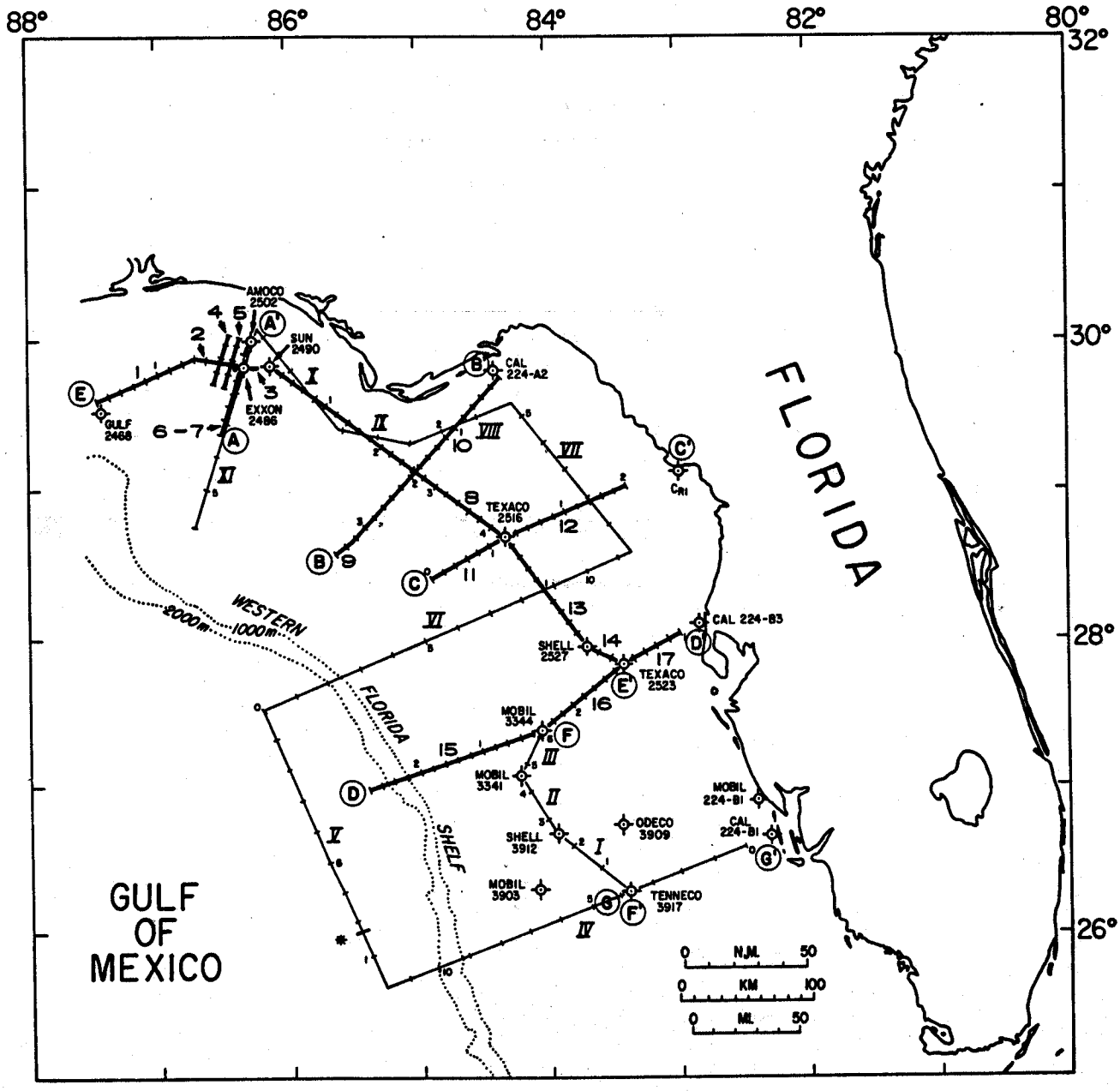
88°
86°
84°
82°
80°
32°
30°
28°
26°
FLORIDA
GULF OF MEXICO
WESTERN
FLORIDA SHELF
5000m
1000m
AMOCO 2502
SUN 2490
EXXON 2486
GULF 2468
CAL 224-A2
TEXACO 2516
CAL 224-B3
SHELL 2527
TEXACO 2523
MOBIL 3344
MOBIL 3341
SHELL 3912
ODECO 3909
MOBIL 3903
TENNECO 3917
MOBIL 224-B1
CAL 224-B1
0 N.M. 50
0 KM 100
0 MI. 50

Figure 1

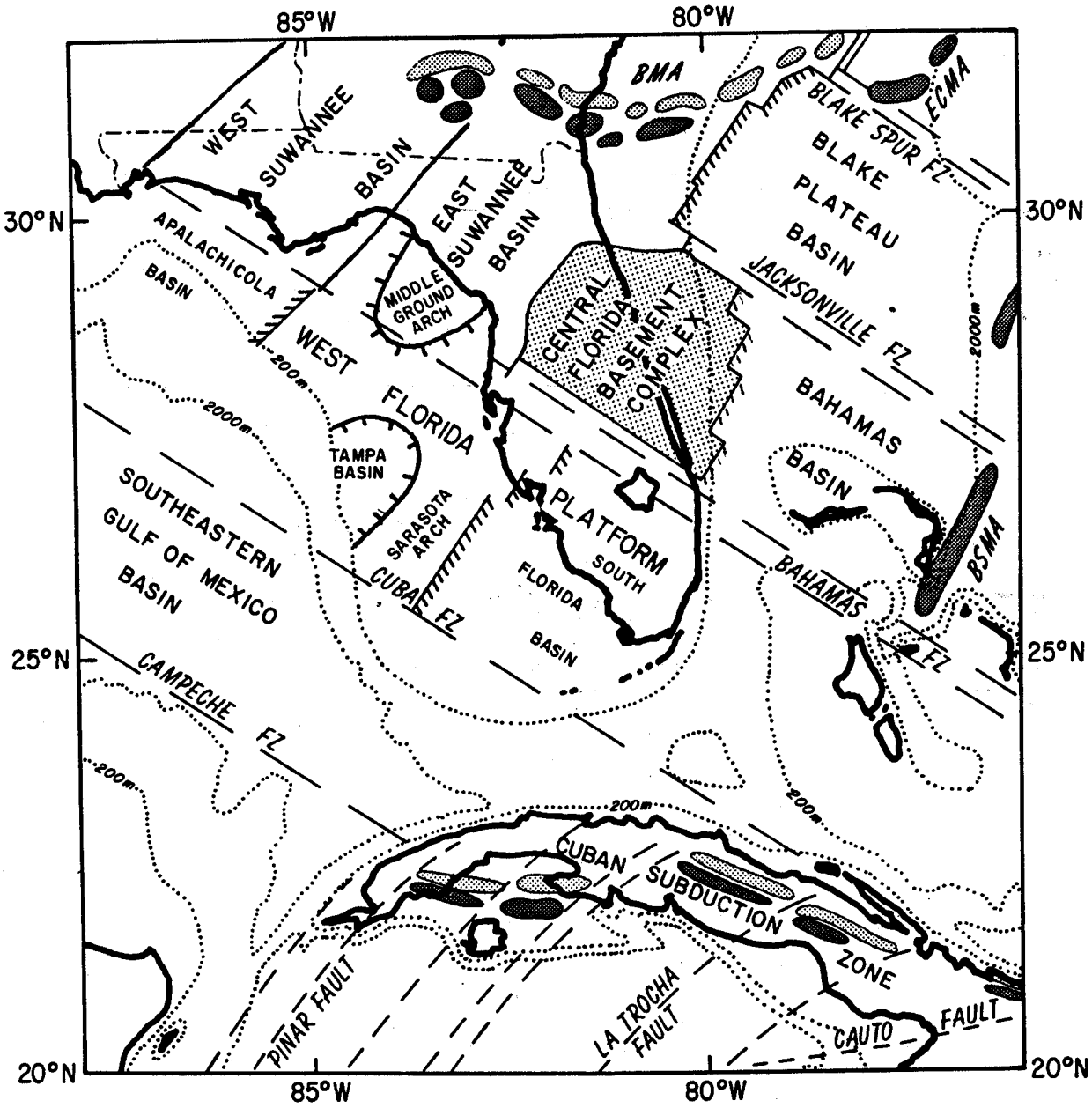
85°W
80°W
30°N
25°N
20°N
WEST SUWANNEE BASIN
EAST SUWANNEE BASIN
BMA
BLAKE SPUR FZ
ECMA
BLAKE PLATEAU BASIN
JACKSONVILLE FZ
APALACHICOLA BASIN
MIDDLE GROUND ARCH
CENTRAL FLORIDA BASEMENT COMPLEX
WEST FLORIDA PLATFORM
TAMPA BASIN
SARASOTA ARCH
SOUTH FLORIDA BASIN
CUBA FZ
BAHAMAS BASIN
BAHAMAS FZ
BSMA
SOUTHEASTERN GULF OF MEXICO BASIN
CAMPECHE FZ
200m
2000m
CUBAN SUBDUCTION ZONE
PINAR FAULT
LA TROCHA FAULT
CAUTO FAULT

Figure 2

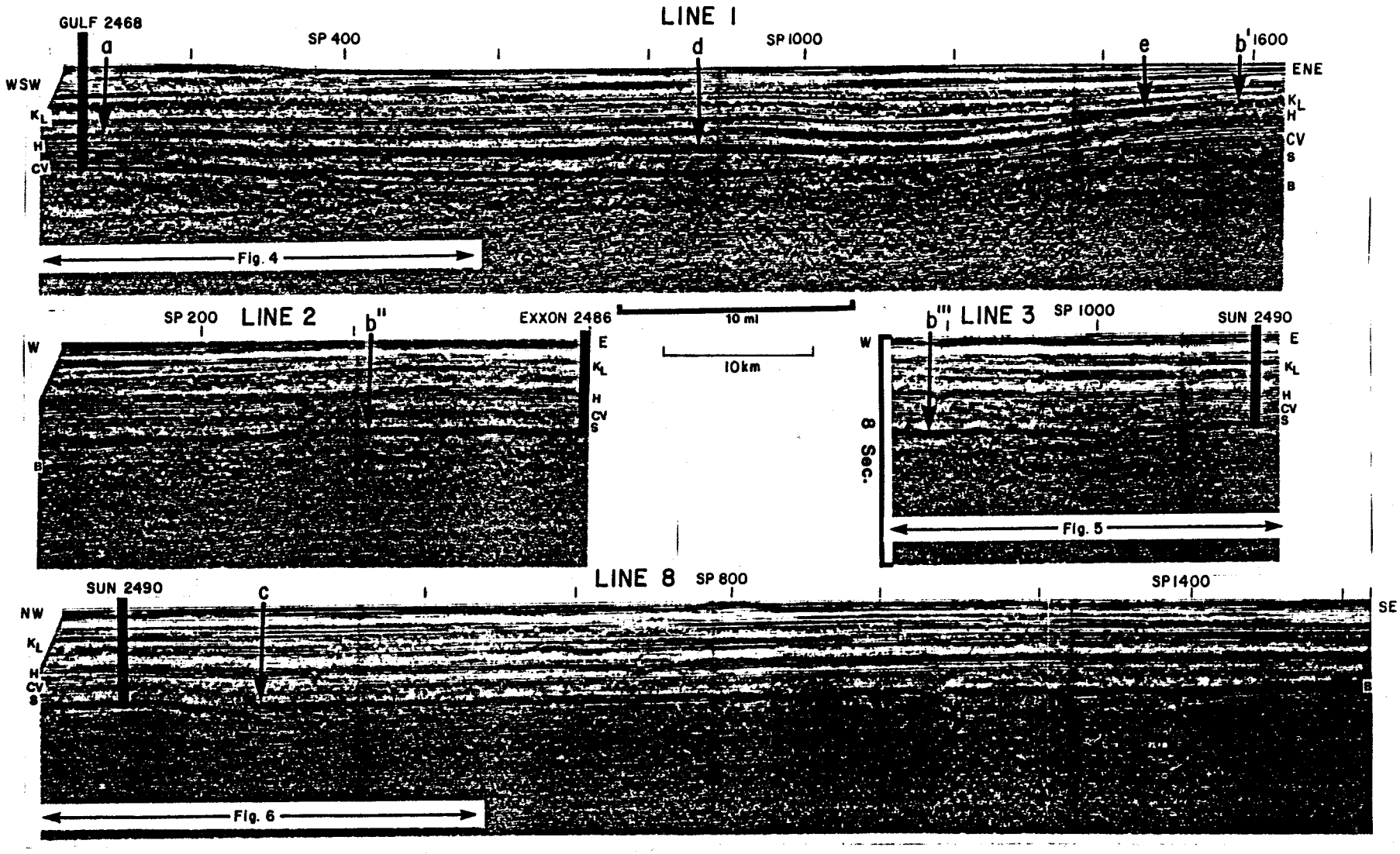
LINE 1
GULF 2468
a
SP 400
d
SP 1000
e
b' 1600
WSW
ENE
KL
H
CV
S
B
Fig. 4
LINE 2
SP 200
b''
EXXON 2486
W
E
10 mi
10 km
LINE 3
b'''
SP 1000
SUN 2490
8 Sec.
Fig. 5
LINE 8
SUN 2490
c
SP 800
SP 1400
NW
SE
Fig. 6

Figure 3

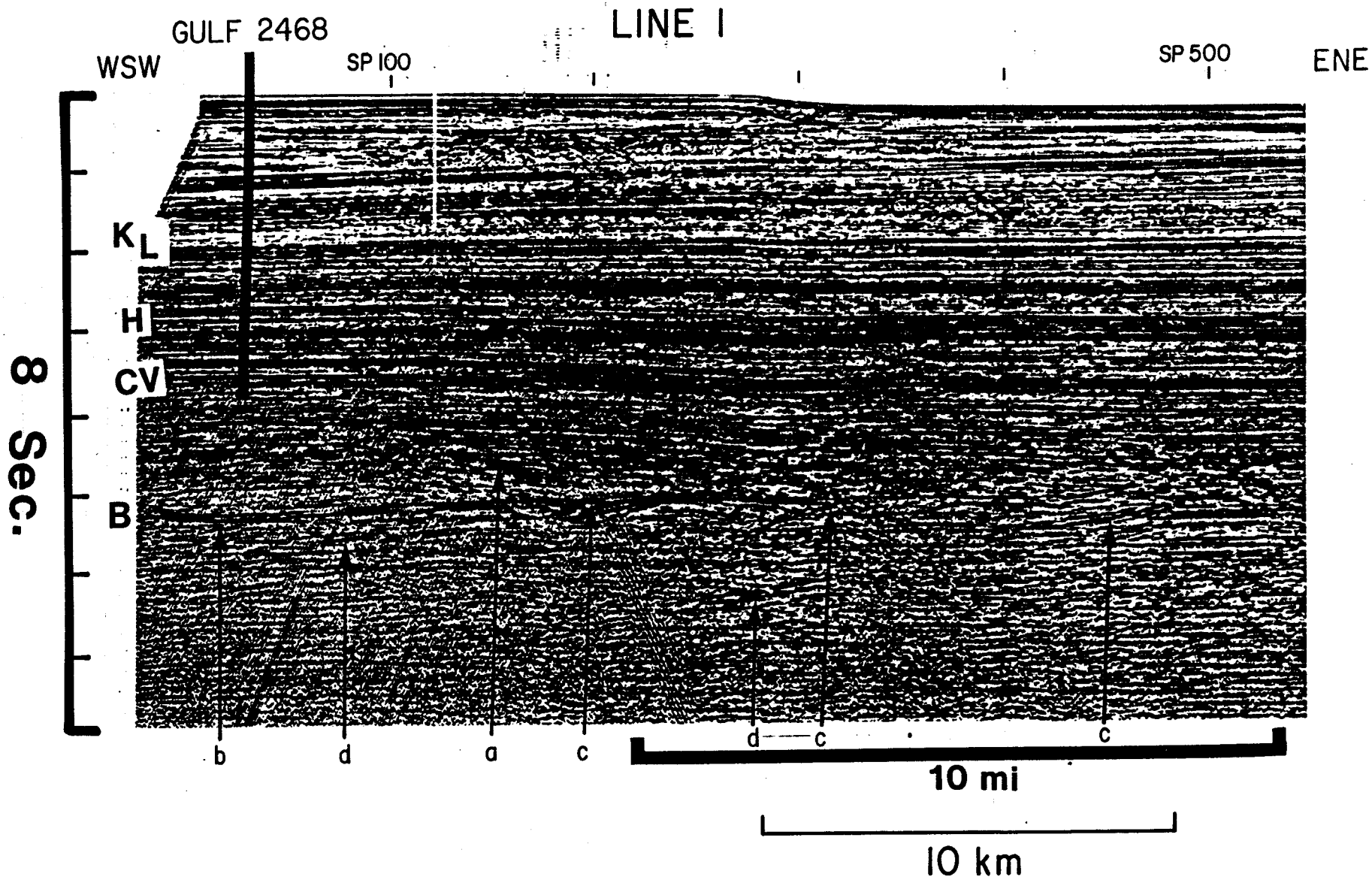
LINE I
GULF 2468
WSW
SP 100
SP 500
ENE
8 Sec.
K
L
H
CV
B
b
d
a
c
d
c
c
10 mi
10 km

Figure 4

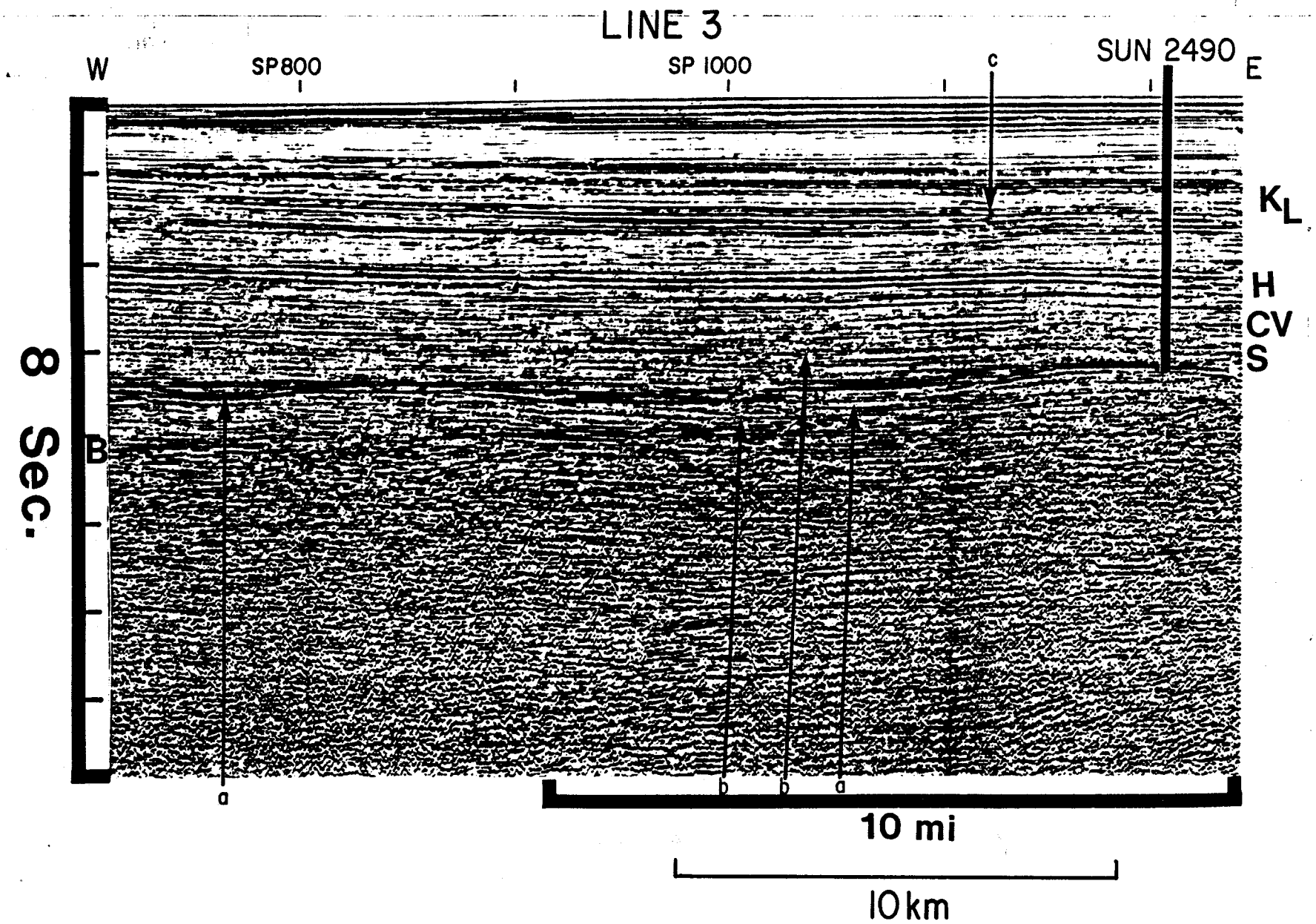

Figure 5

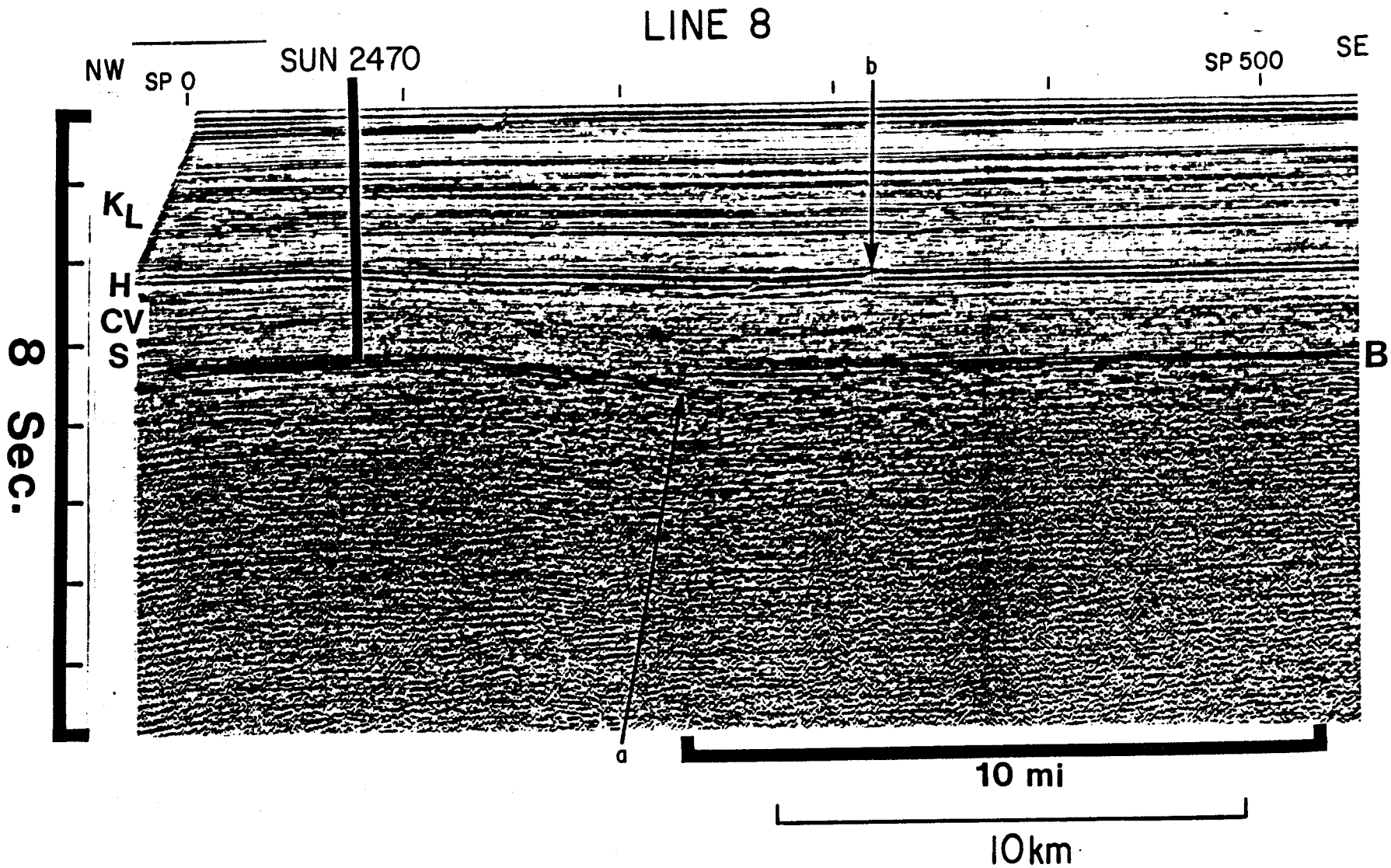

Figure 6

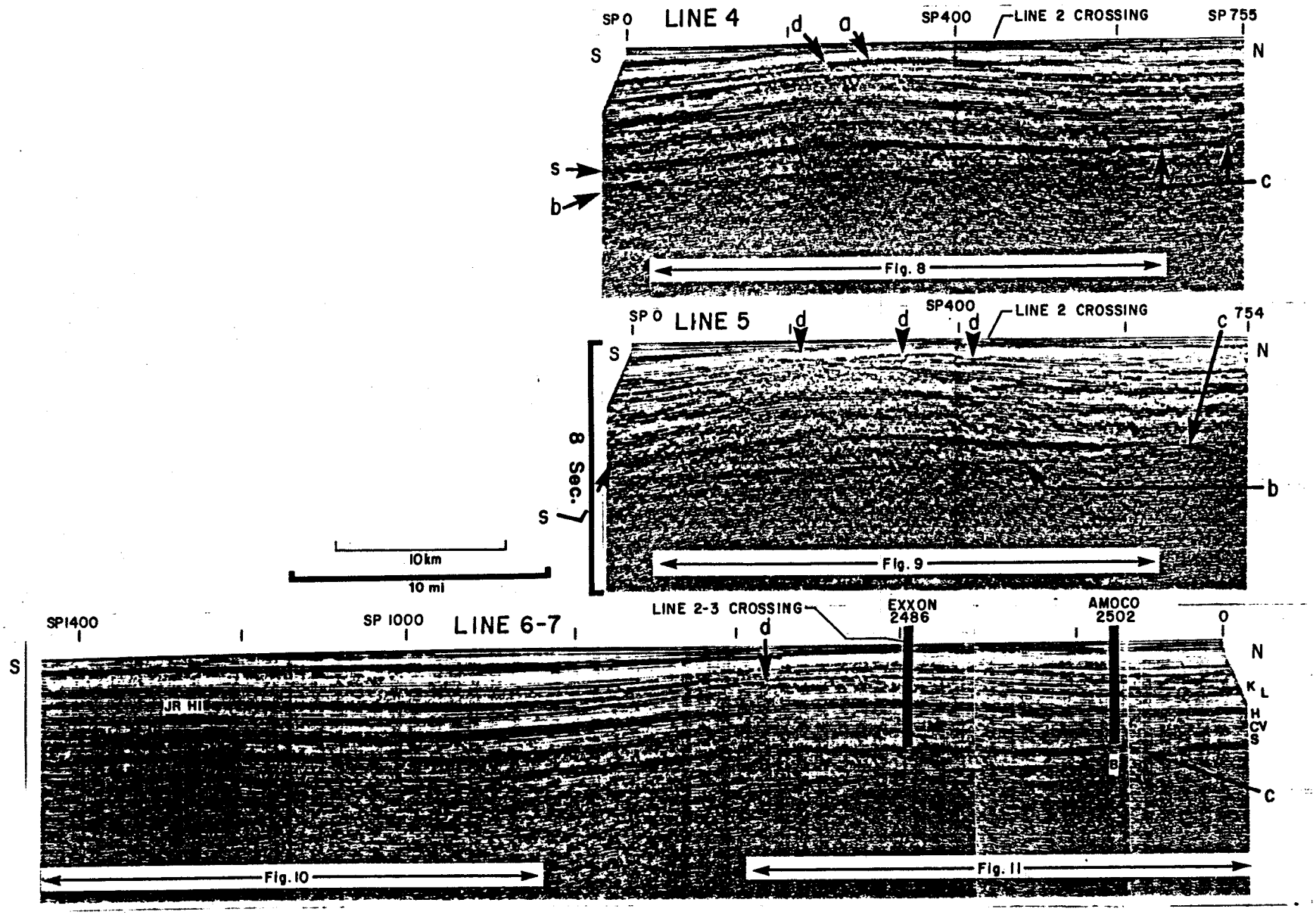
LINE 4
SP 0
SP400
LINE 2 CROSSING
SP 755
S
N
d
a
s
b
c
Fig. 8
LINE 5
SP 0
SP400
LINE 2 CROSSING
754
d
d
d
c
b
8 Sec.
10km
10 mi
Fig. 9
LINE 6-7
SP1400
SP 1000
LINE 2-3 CROSSING
EXXON 2486
AMOCO 2502
0
d
JR HI
K
L
H
CV
S
B
c
Fig. 10
Fig. 11

Figure 7

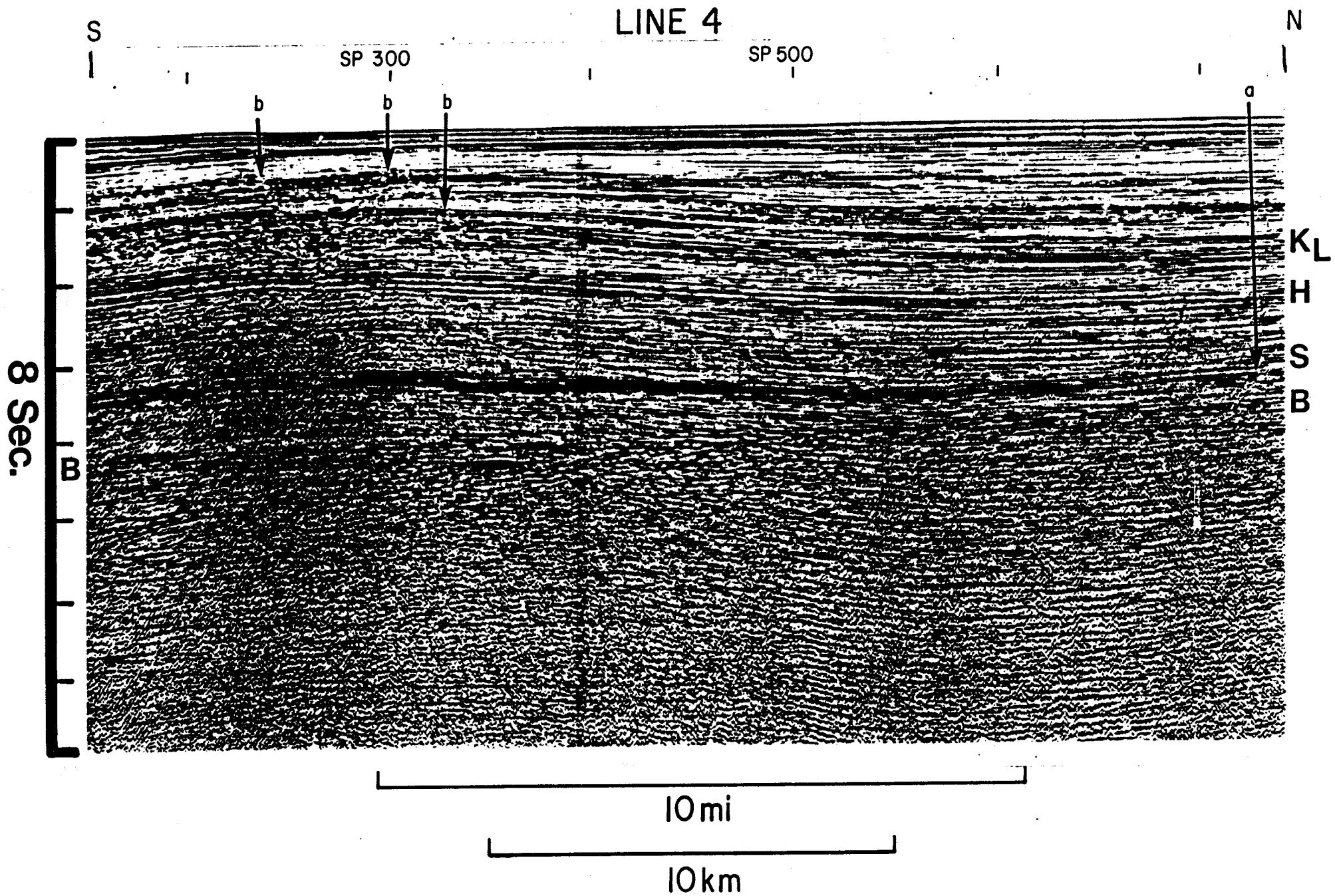

Figure 8

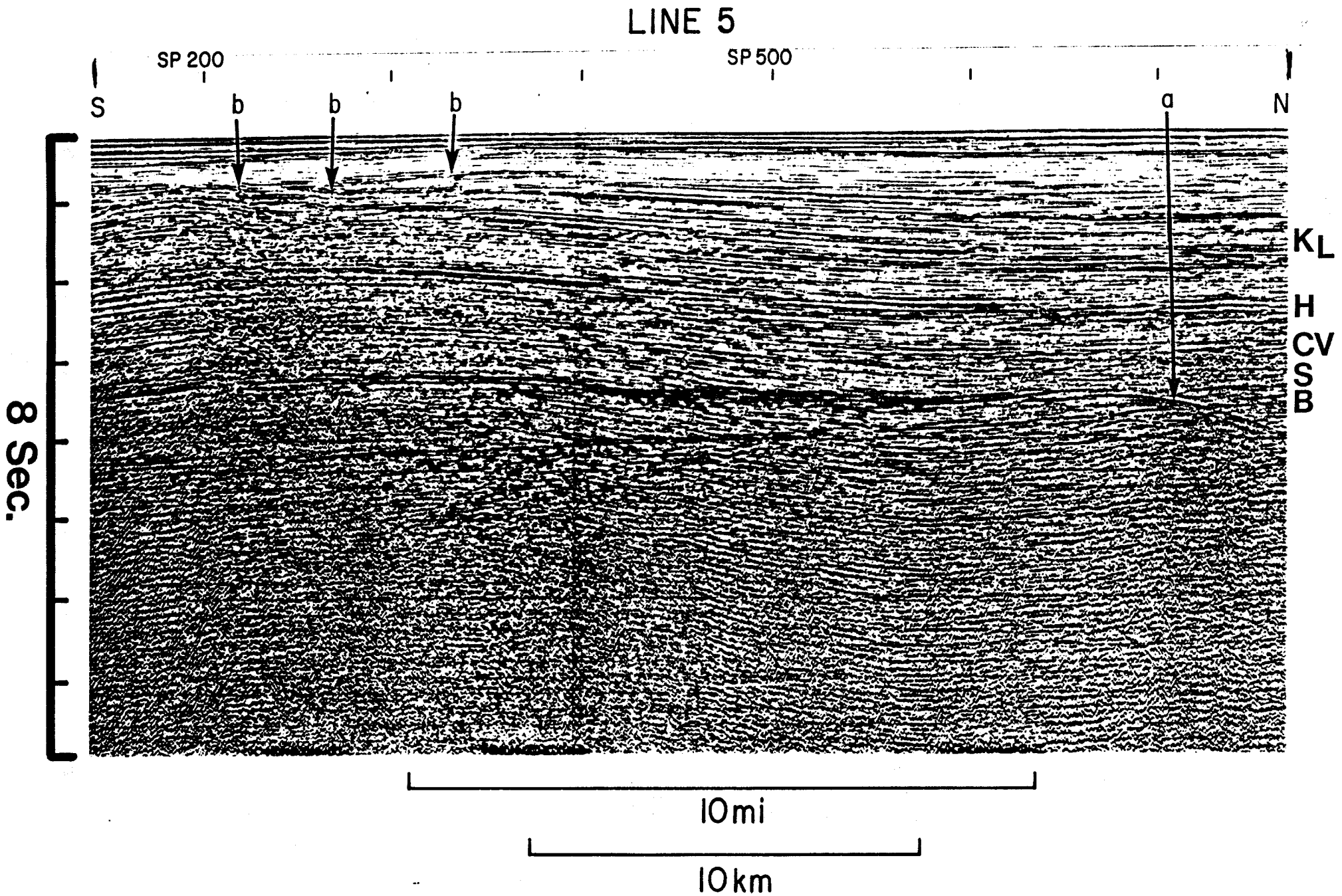

Figure 9

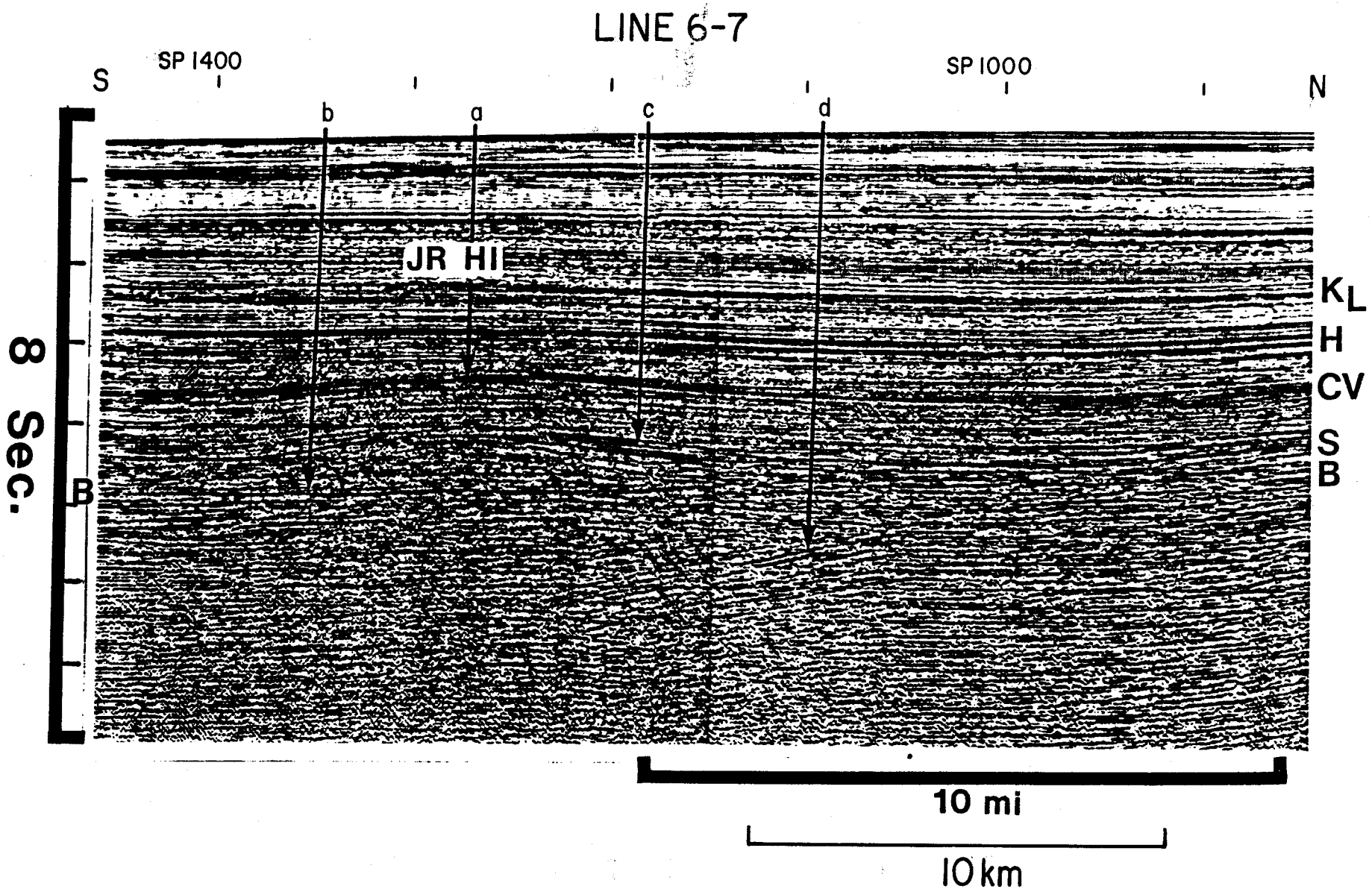

Figure 10

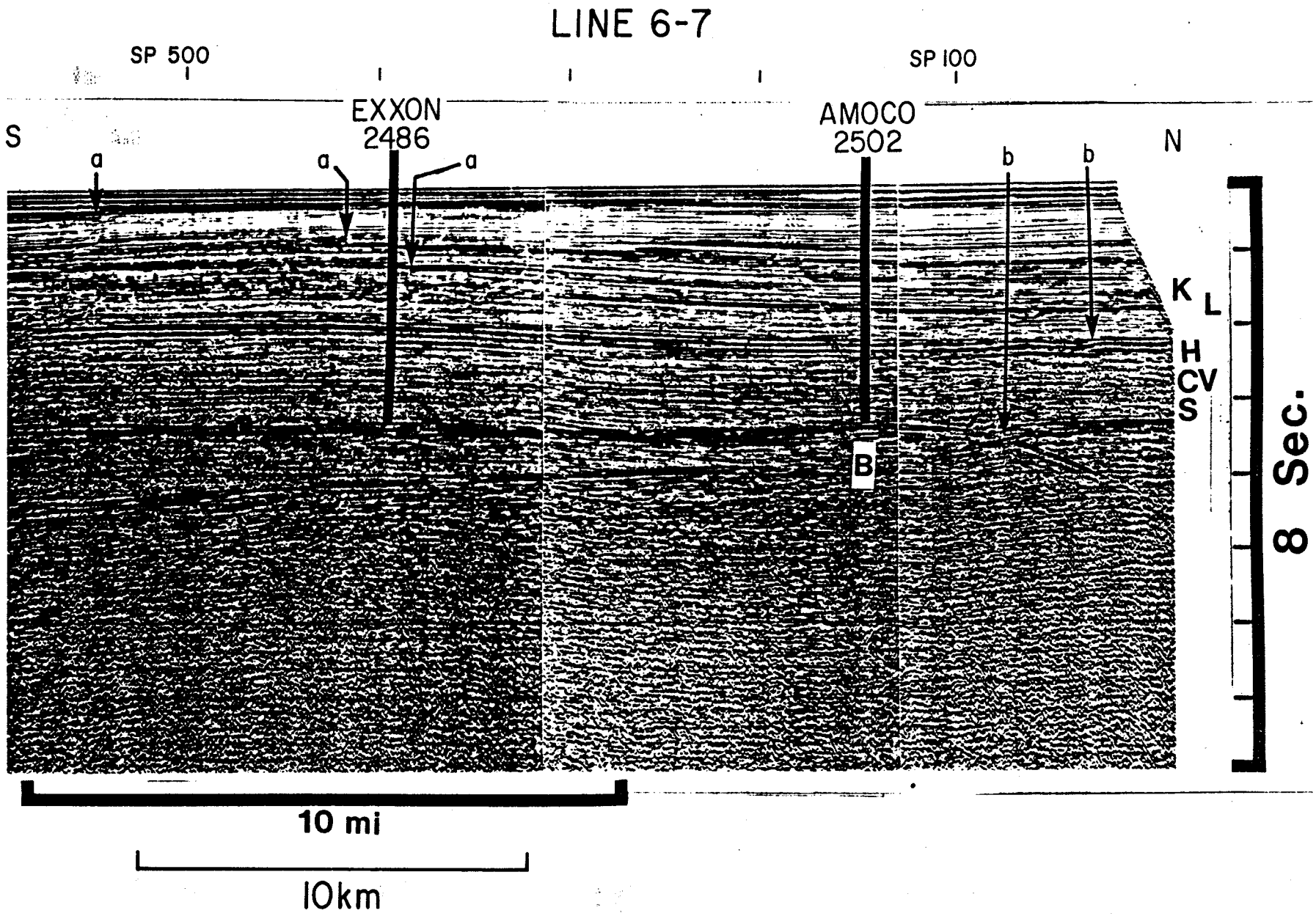
LINE 6-7
SP 500
SP 100
S
N
EXXON
2486
AMOCO
2502
a
a
a
b
b
B
K
L
H
CV
S
8 Sec.
10 mi
10km

Figure II

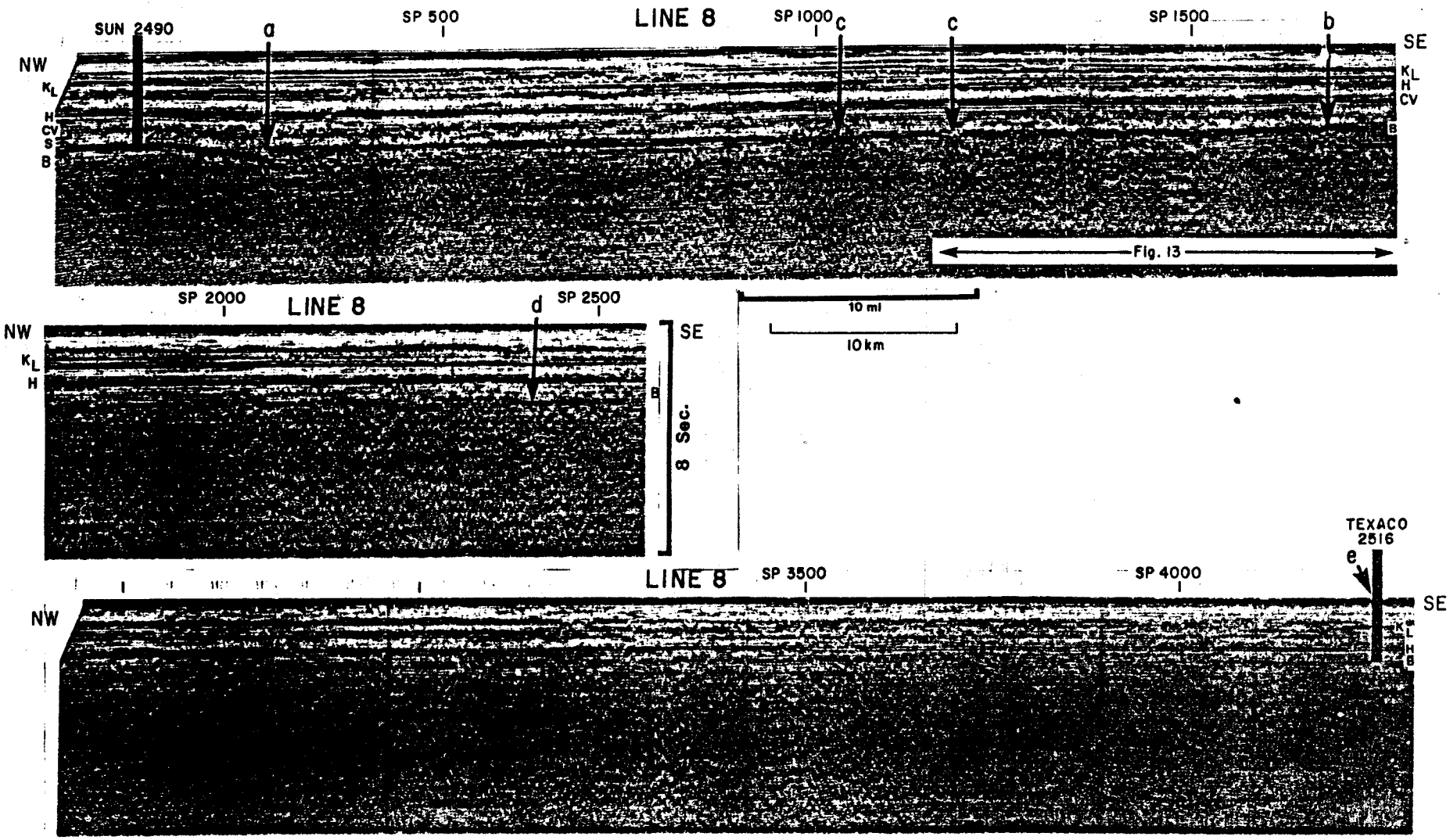
LINE 8
SUN 2490
a
SP 500
SP 1000
c
c
SP 1500
b
NW
SE
KL
H
CV
S
B
Fig. 13
SP 2000
LINE 8
d
SP 2500
NW
SE
KL
H
B
8 Sec.
10 mi
10 km
TEXACO
2516
e
LINE 8
SP 3500
SP 4000
NW
SE
KL
H
B

Figure 12

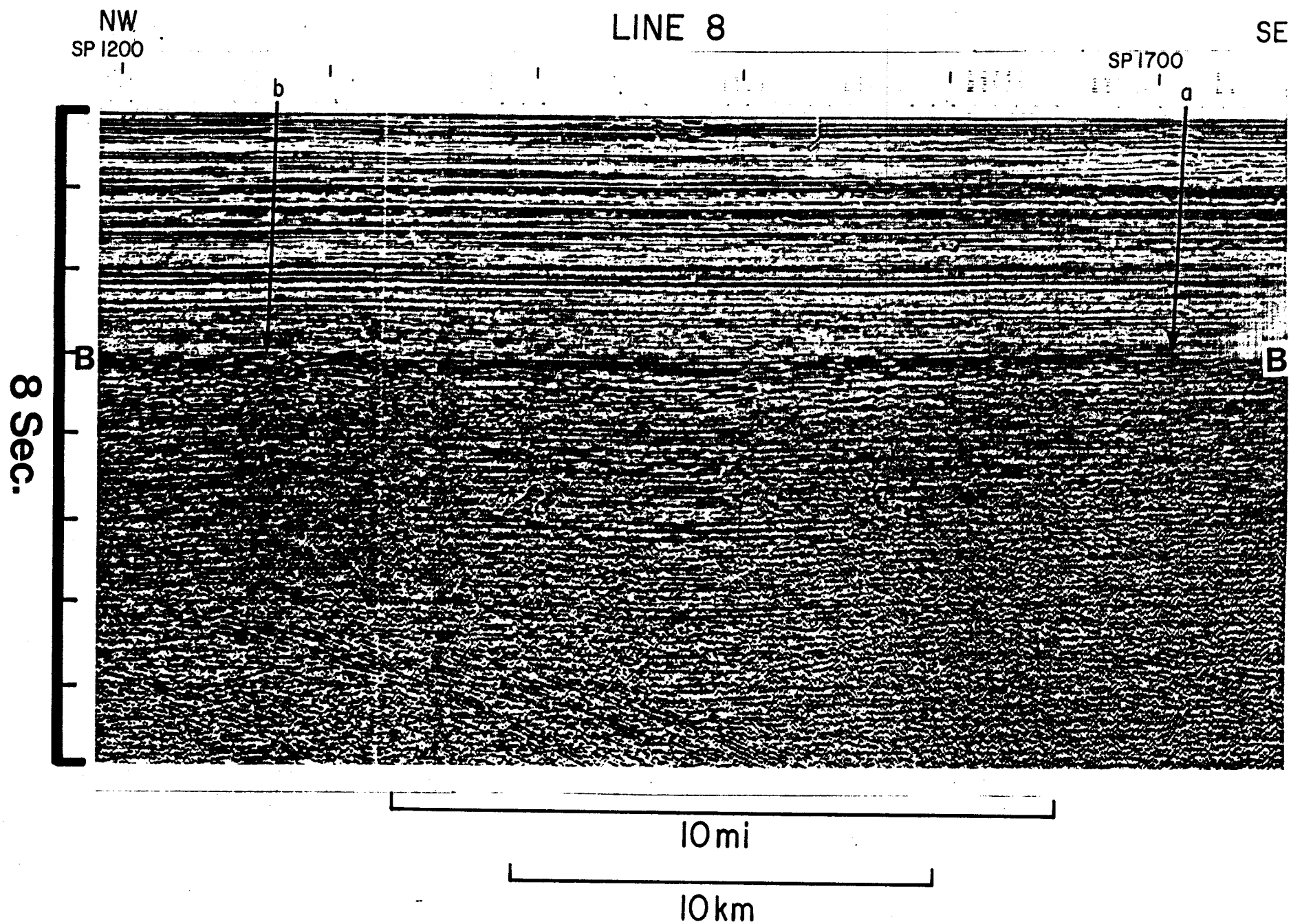

Figure 13

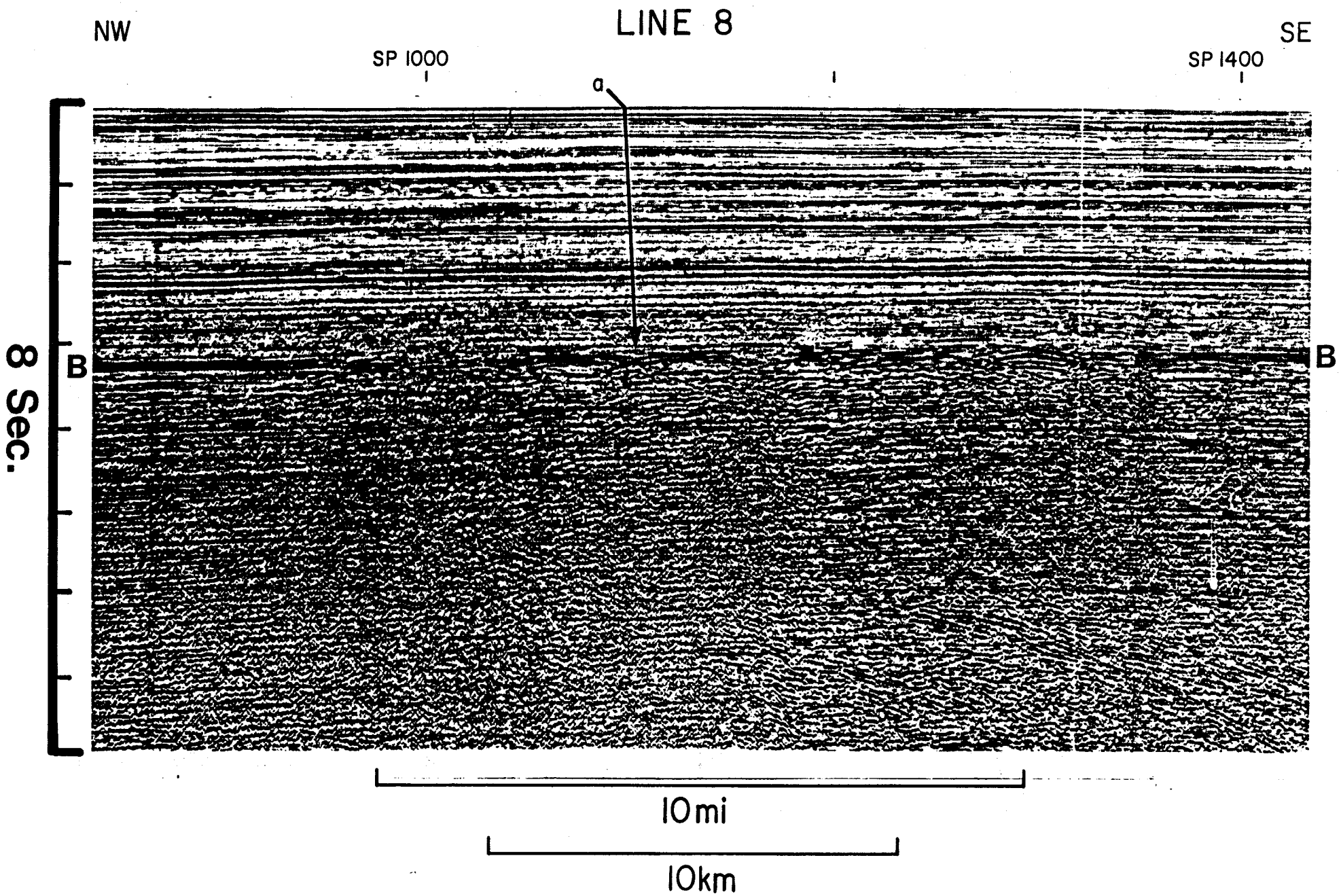

Figure 14

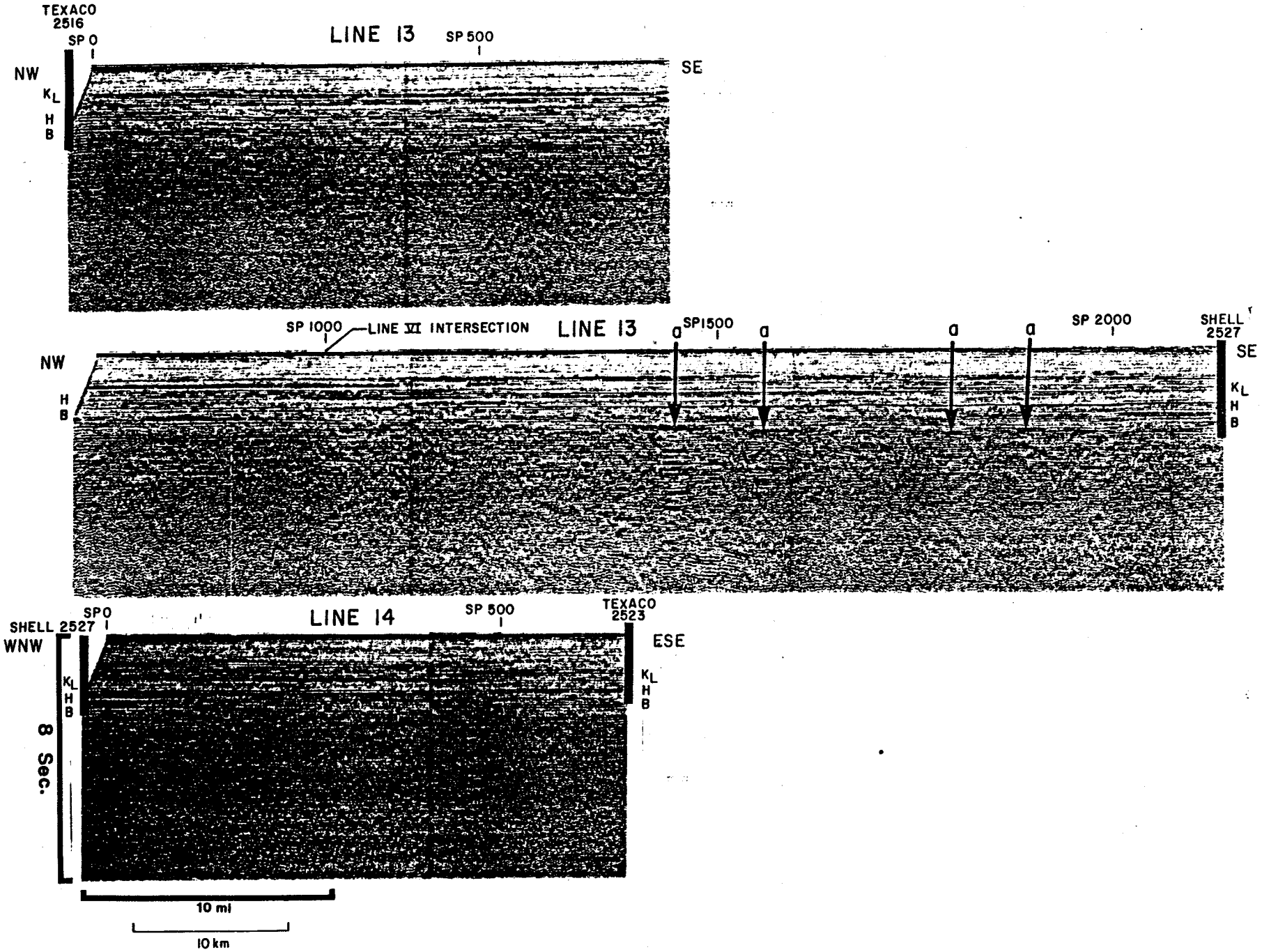
TEXACO
2516
SP 0
LINE 13
SP 500
NW
SE
KL
H
B
SP 1000
LINE VI INTERSECTION
LINE 13
SP1500
SP 2000
SHELL
2527
NW
SE
H
B
KL
H
B
SHELL 2527
SP0
LINE 14
SP 500
TEXACO
2523
WNW
ESE
KL
H
B
KL
H
B
8 Sec.
10 mi
10 km

Figure 15

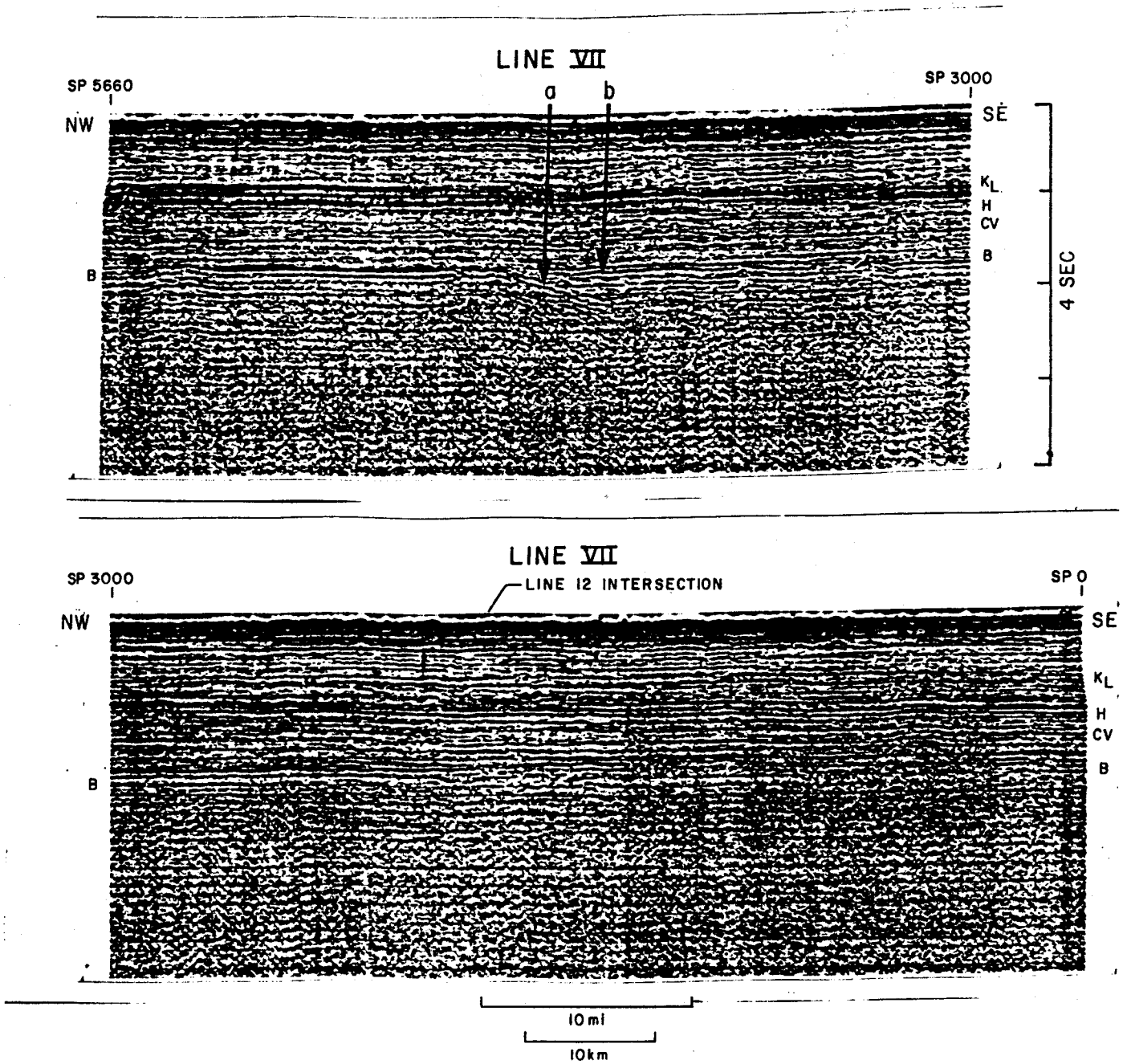
LINE VII
SP 5660
NW
a
b
SP 3000
SE
KL
H
CV
B
B
4 SEC
LINE VII
SP 3000
NW
LINE 12 INTERSECTION
SP 0
SE
KL
H
CV
B
B
10 mi
10 km

Figure 16

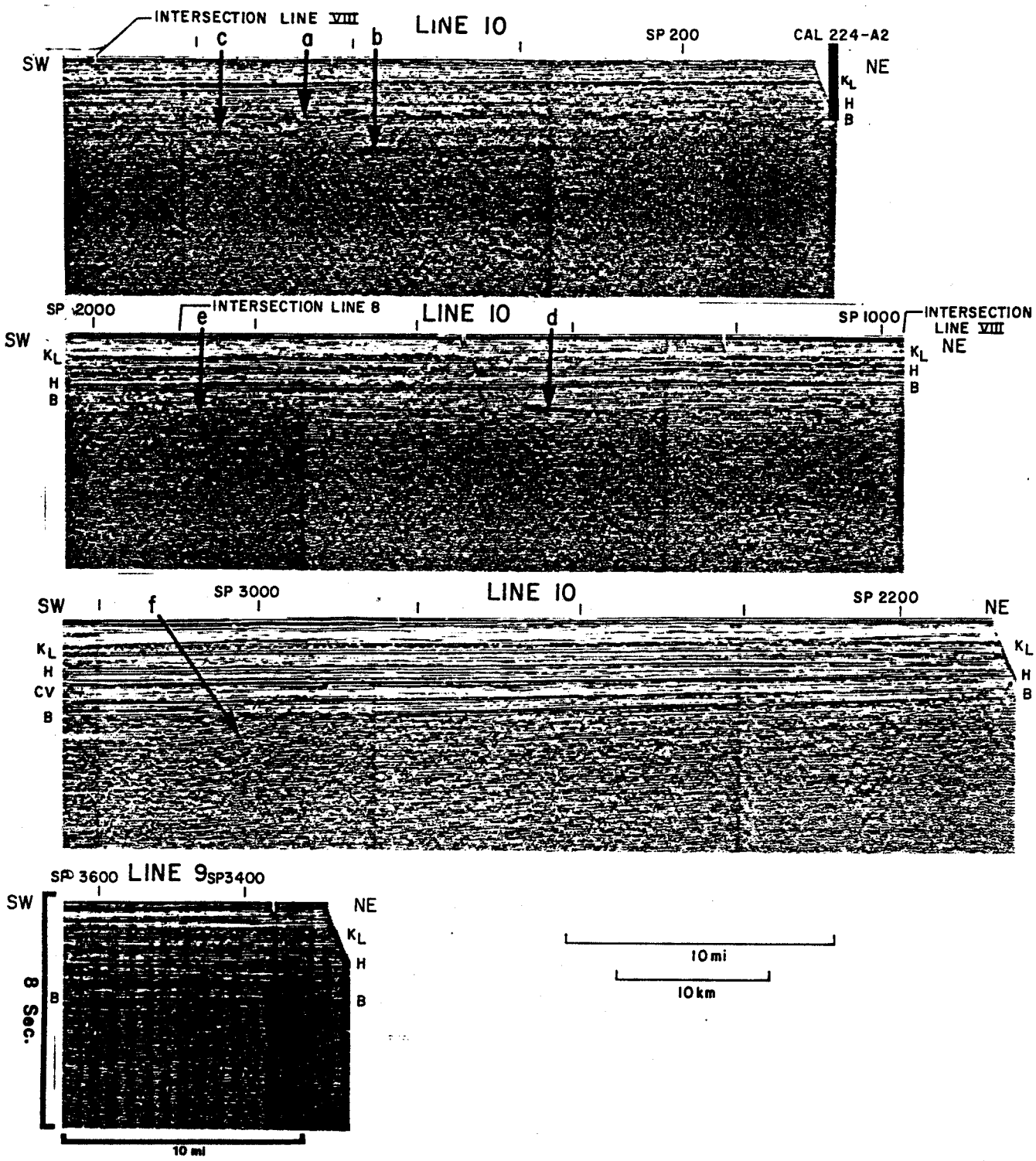
INTERSECTION LINE VIII
LINE 10
SP 200
CAL 224-A2
SW
NE
c
a
b
K_L
H
B
SP 2000
INTERSECTION LINE 8
LINE 10
d
SP 1000
INTERSECTION LINE VIII
SW
NE
K_L
H
B
e
LINE 10
SP 3000
SP 2200
SW
NE
f
K_L
H
CV
B
SP 3600
LINE 9
SP3400
SW
NE
K_L
H
B
8 Sec.
10 mi
10 mi
10 km

Figure 17

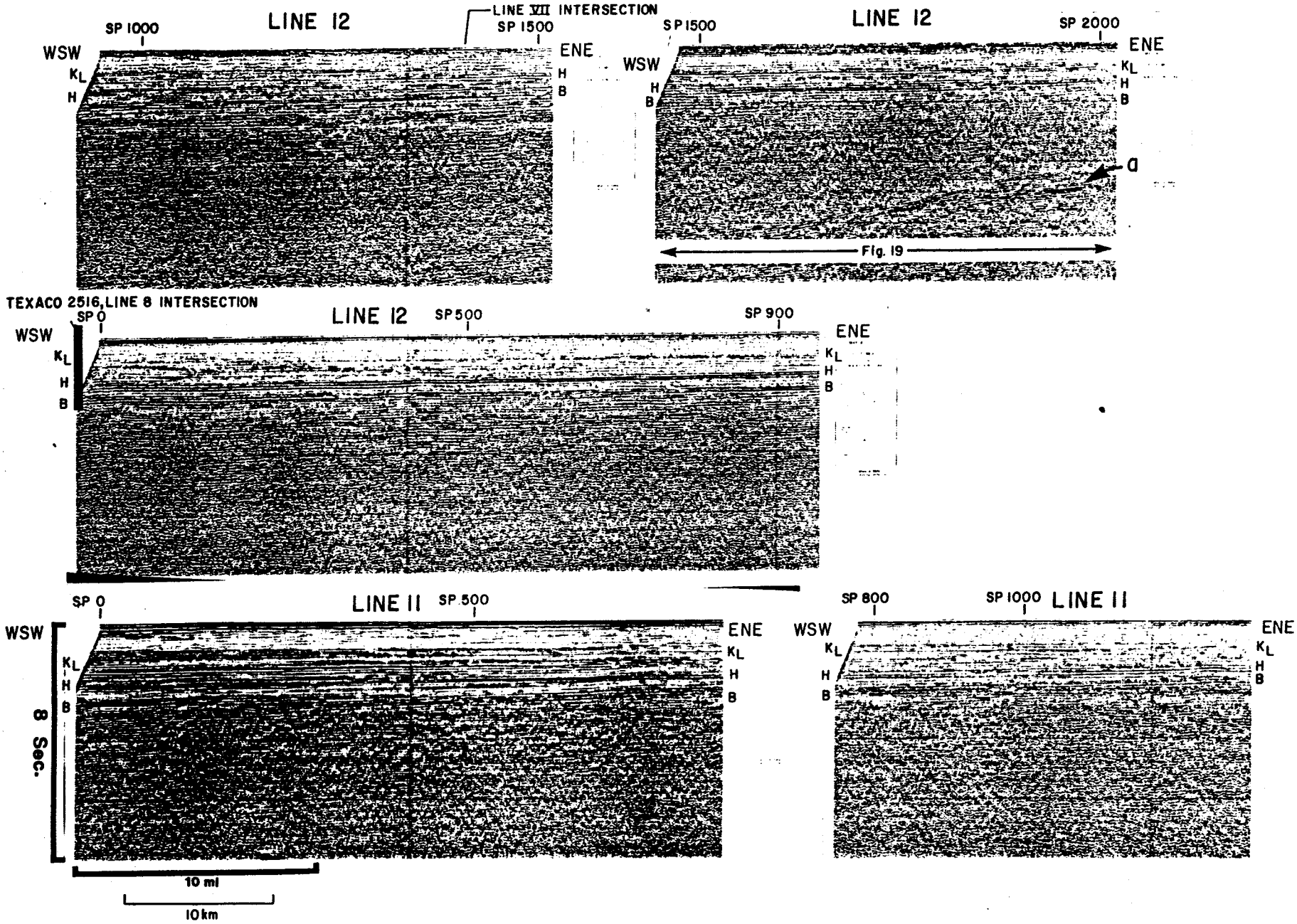
LINE 12
SP 1000
LINE VII INTERSECTION
SP 1500
WSW
ENE
KL
H
B
LINE 12
SP 1500
SP 2000
a
Fig. 19
TEXACO 2516, LINE 8 INTERSECTION
SP 0
LINE 12
SP 500
SP 900
LINE 11
SP 0
SP 500
8 Sec.
10 mi
10 km
SP 800
SP 1000
LINE 11

Figure 18

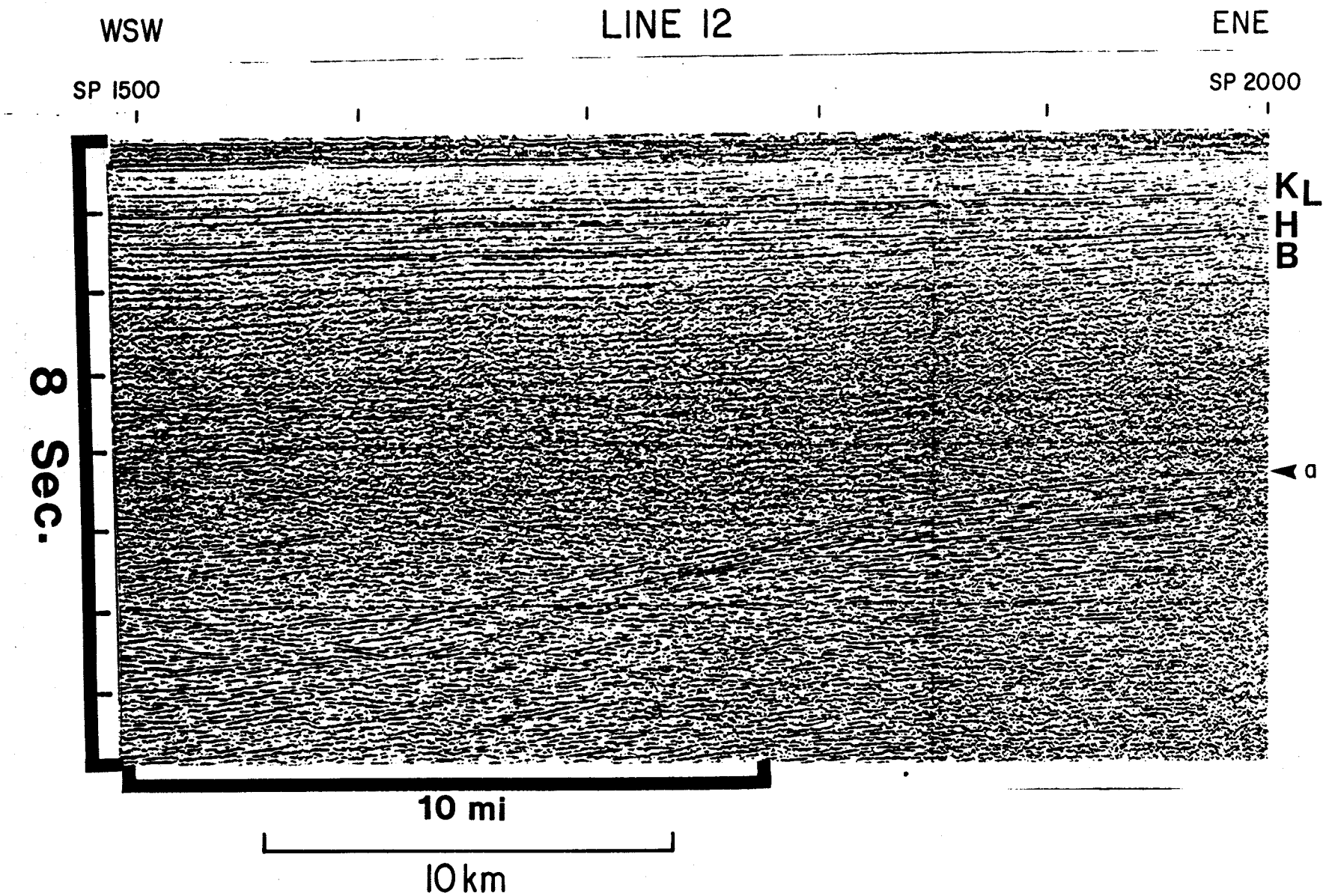

Figure 19

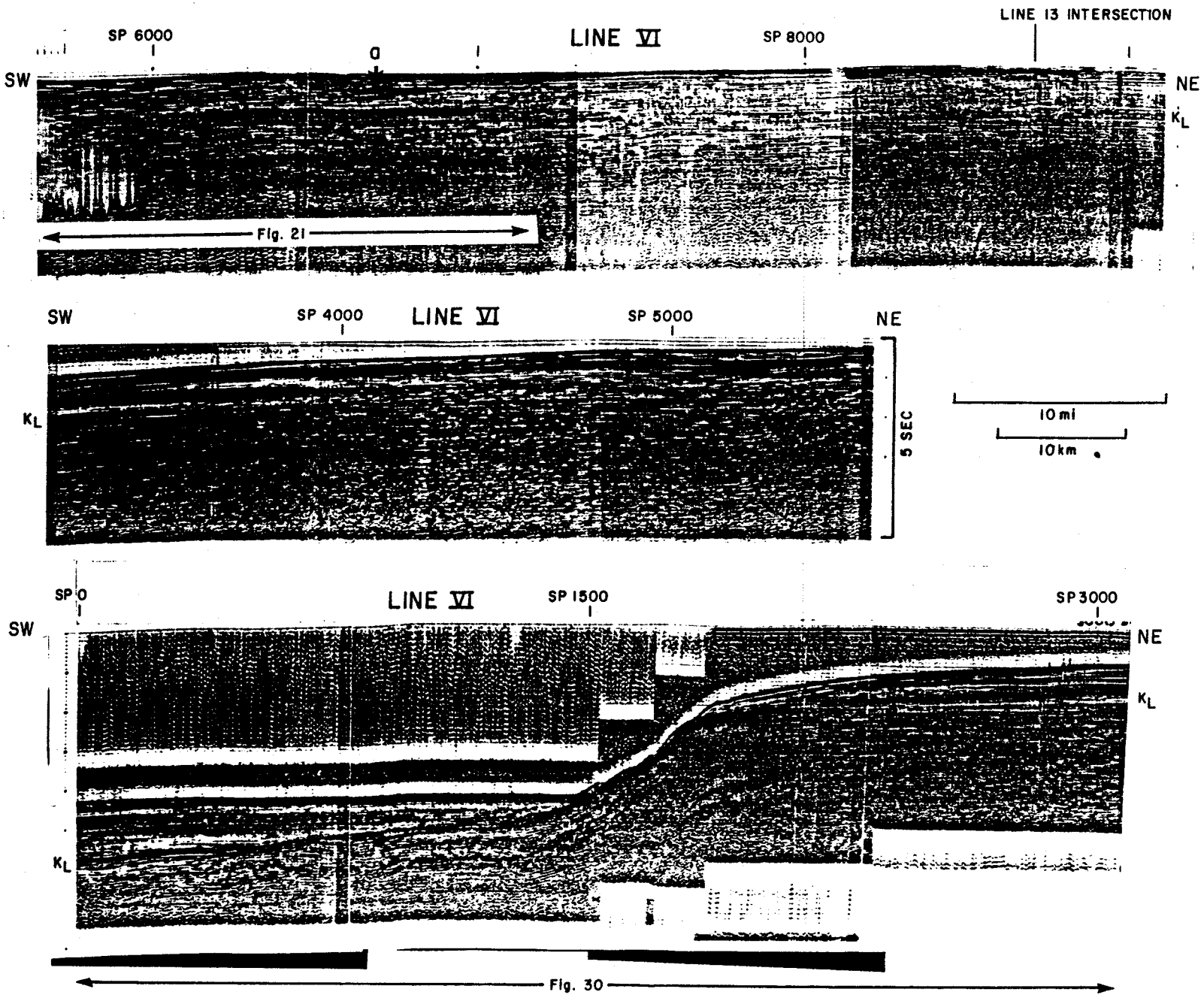
LINE 13 INTERSECTION
SP 6000
LINE VI
SP 8000
SW
NE
K_L
Fig. 21
SW
SP 4000
LINE VI
SP 5000
NE
K_L
5 SEC
10 mi
10 km
SP 0
LINE VI
SP 1500
SP 3000
SW
NE
K_L
K_L
Fig. 30

Figure 20

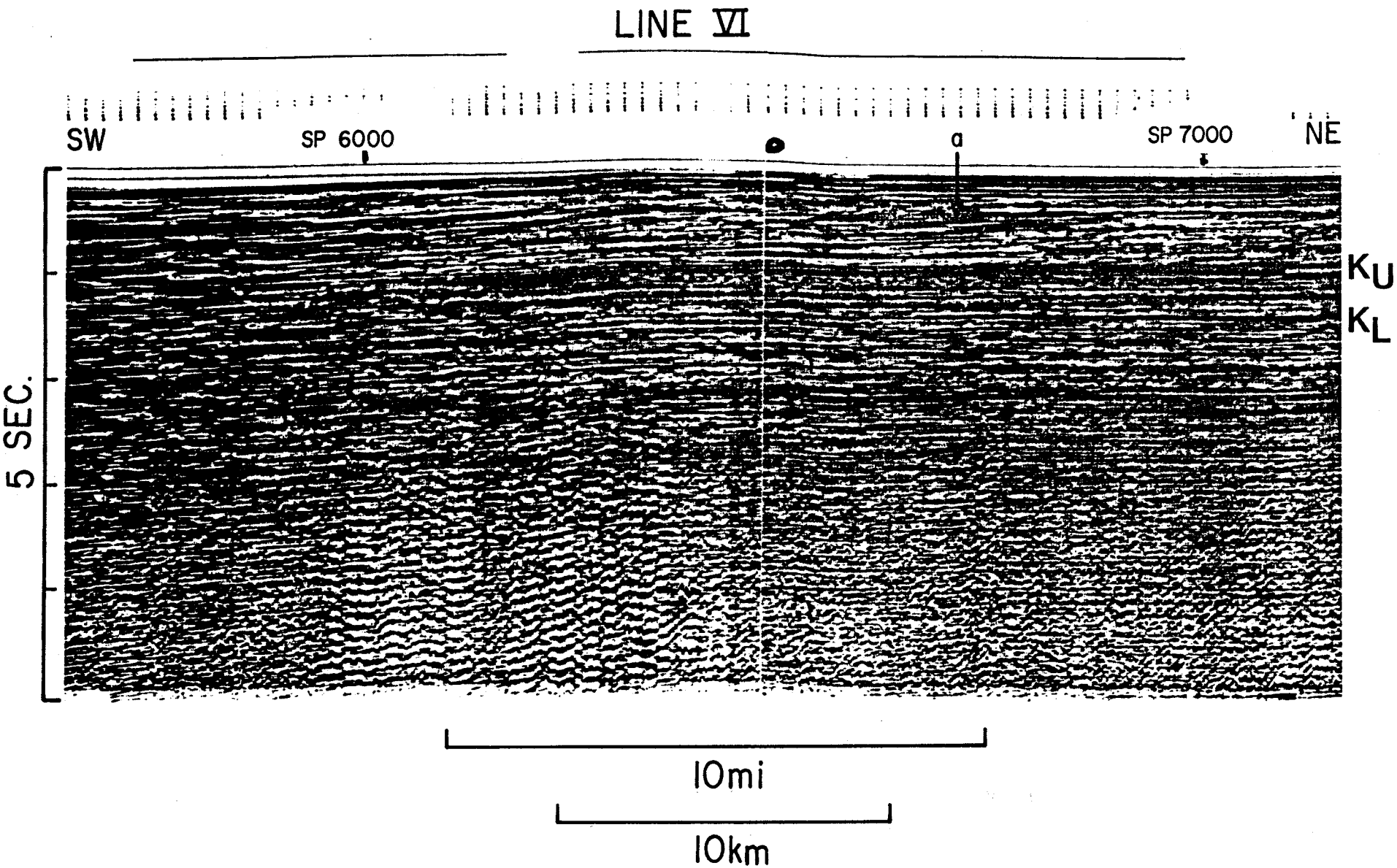

Figure 21

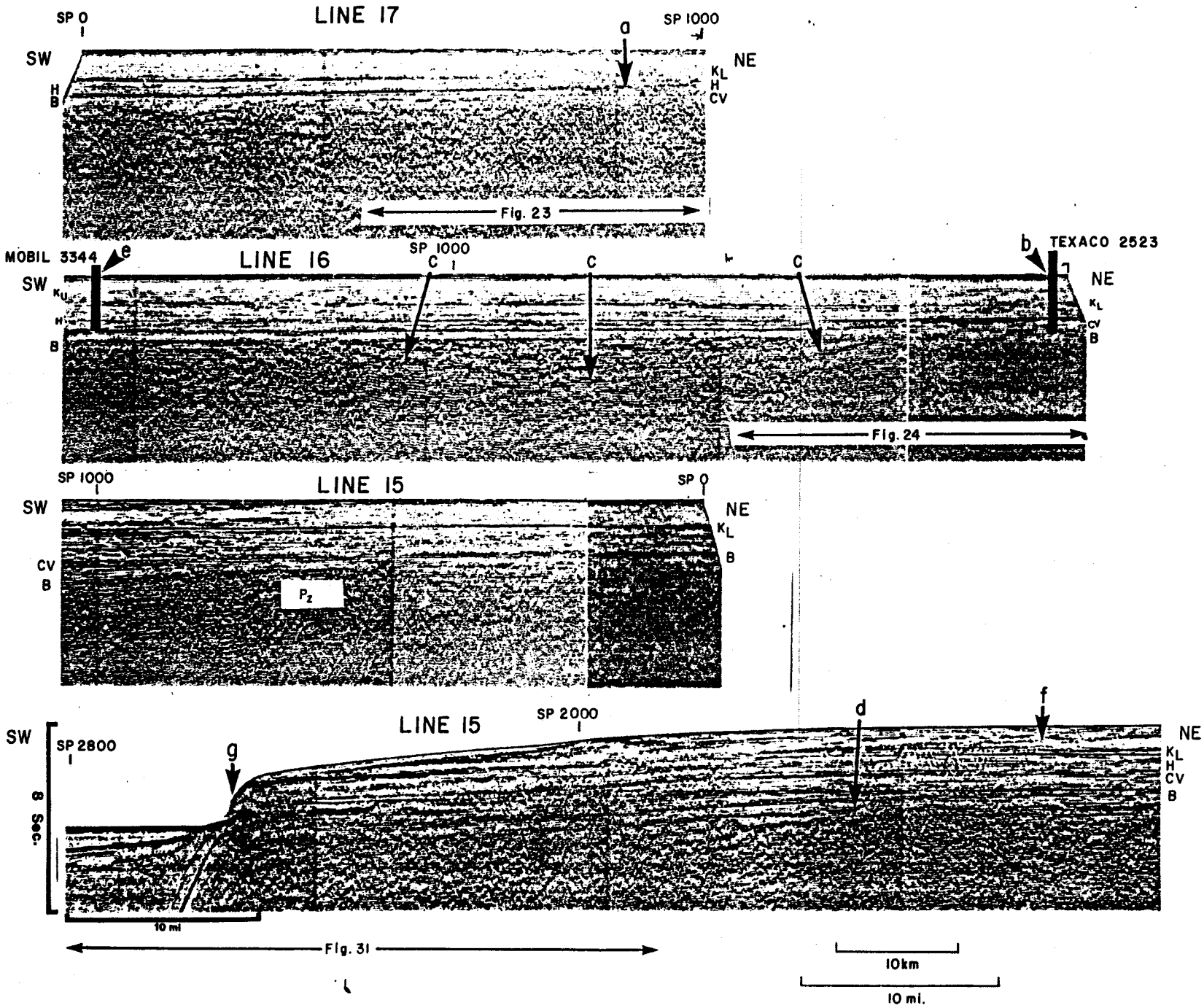
LINE 17
SP 0
SP 1000
a
SW
NE
H
B
KL
H
CV
Fig. 23
MOBIL 3344
e
LINE 16
SP 1000
c
c
c
b
TEXACO 2523
SW
NE
KU
H
B
KL
CV
B
Fig. 24
SP 1000
LINE 15
SP 0
SW
NE
KL
B
CV
B
Pz
LINE 15
SP 2000
d
f
SW
SP 2800
g
NE
KL
H
CV
B
8 Sec.
10 mi
Fig. 31
10km
10 mi.

Figure 22

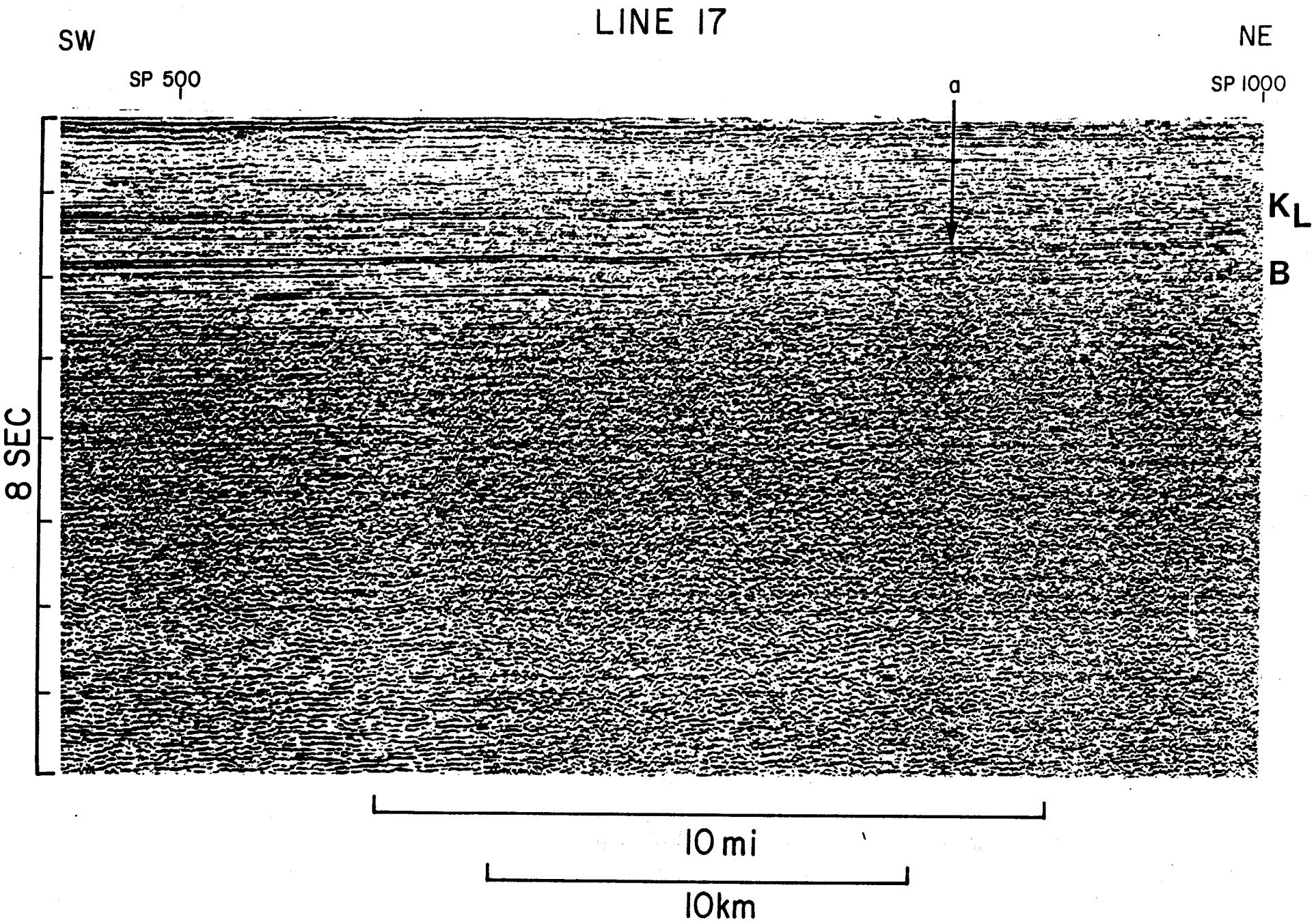

Figure 23

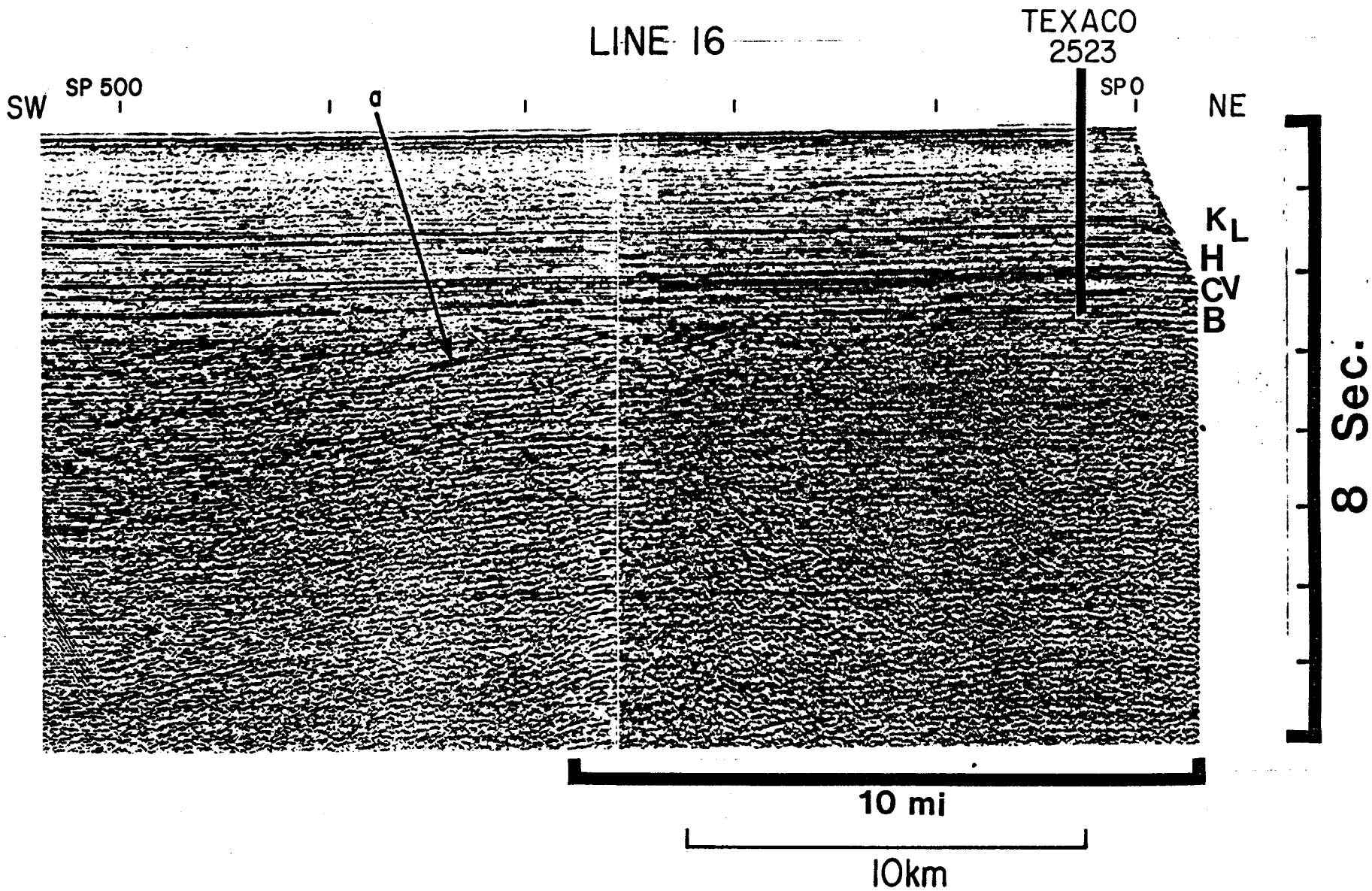

Figure 24

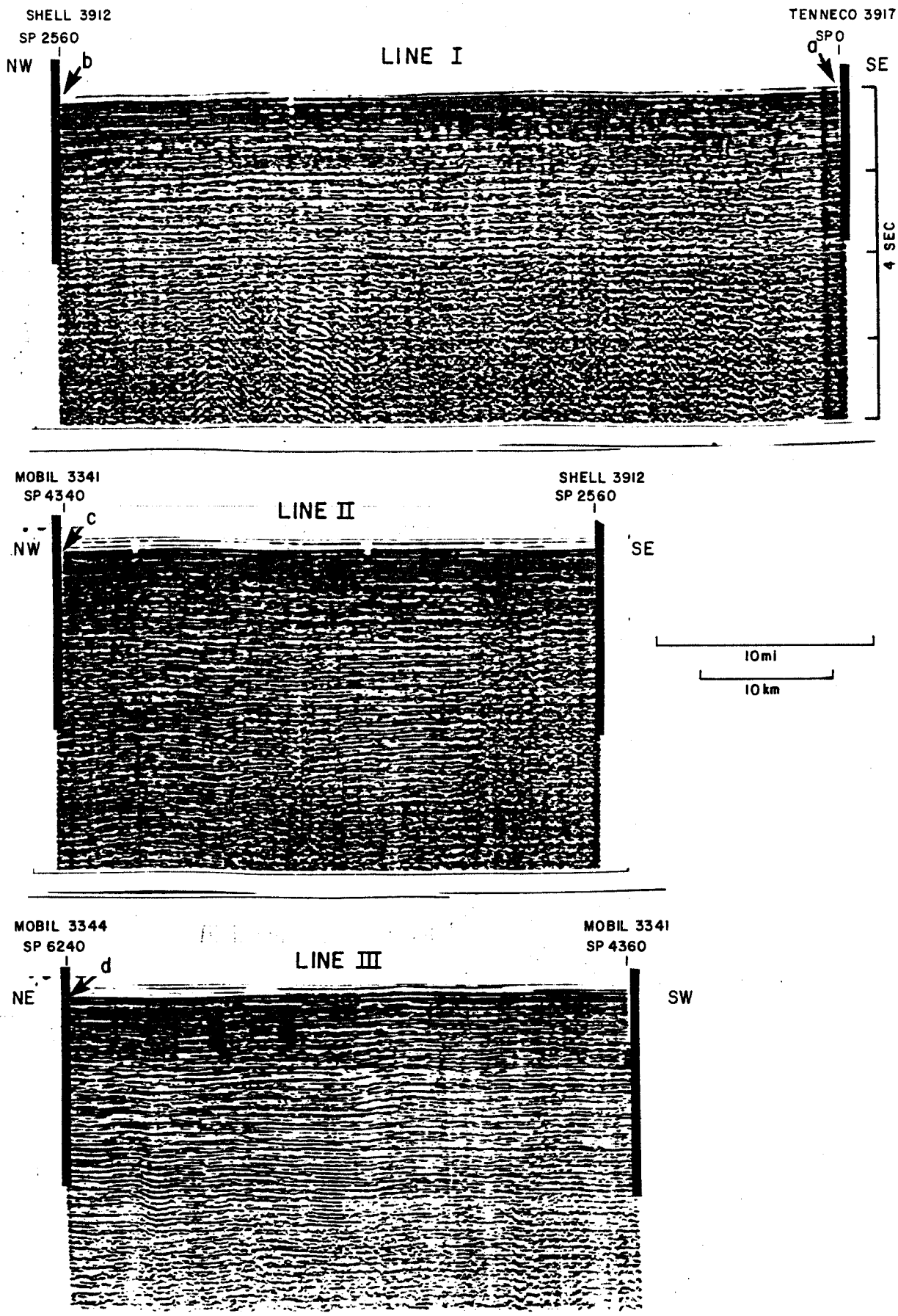
SHELL 3912
SP 2560
NW
b
LINE I
TENNECO 3917
SP 0
a
SE
4 SEC
MOBIL 3341
SP 4340
c
NW
LINE II
SHELL 3912
SP 2560
SE
10 mi
10 km
MOBIL 3344
SP 6240
d
NE
LINE III
MOBIL 3341
SP 4360
SW

Figure 25

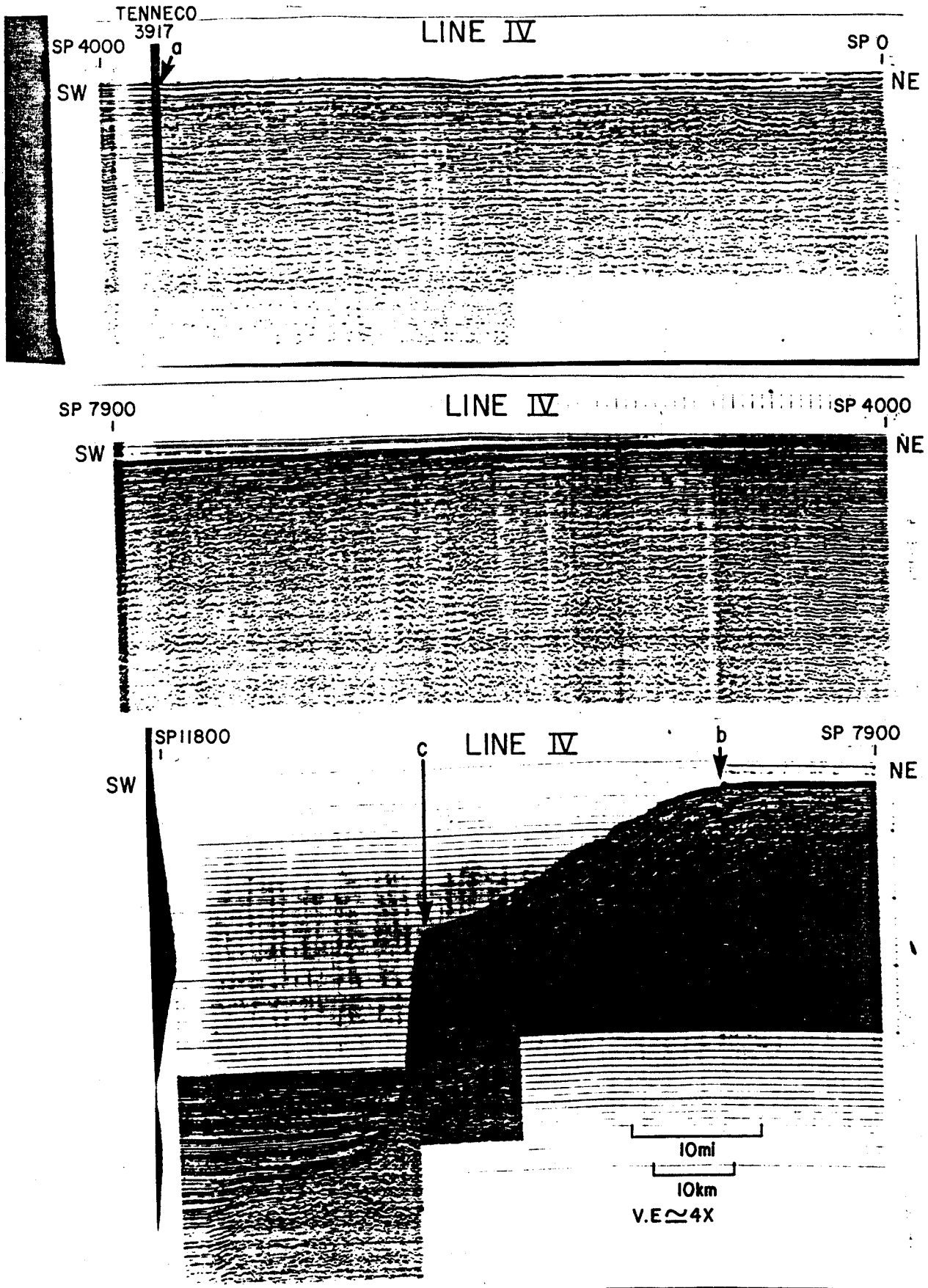

Fig. 29

Figure 26

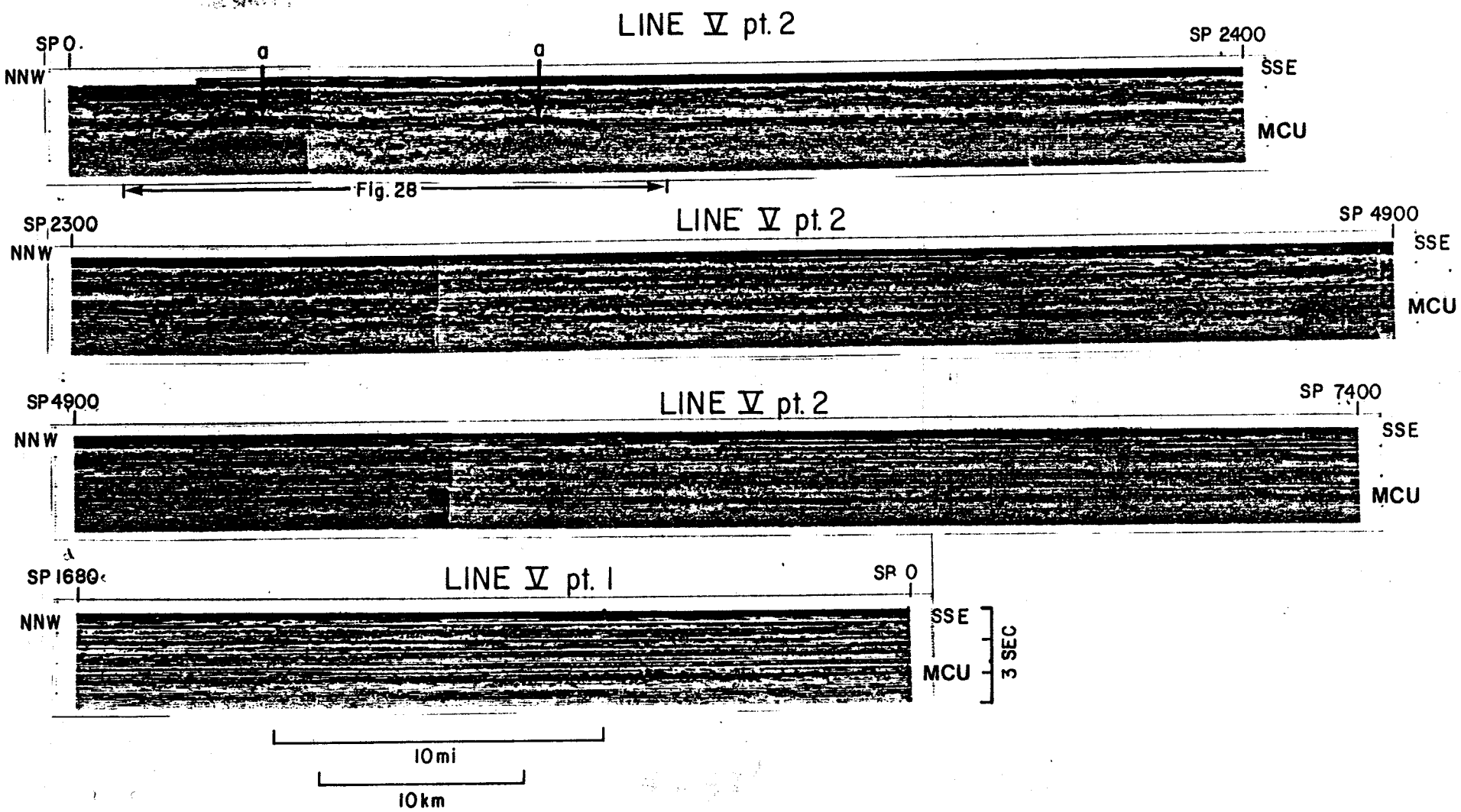
LINE V pt. 2
SP 0
SP 2400
NNW
SSE
a
a
MCU
Fig. 28
LINE V pt. 2
SP 2300
SP 4900
NNW
SSE
MCU
LINE V pt. 2
SP 4900
SP 7400
NNW
SSE
MCU
LINE V pt. 1
SP 1680
SP 0
NNW
SSE
MCU
3 SEC
10 mi
10 km

Figure 27

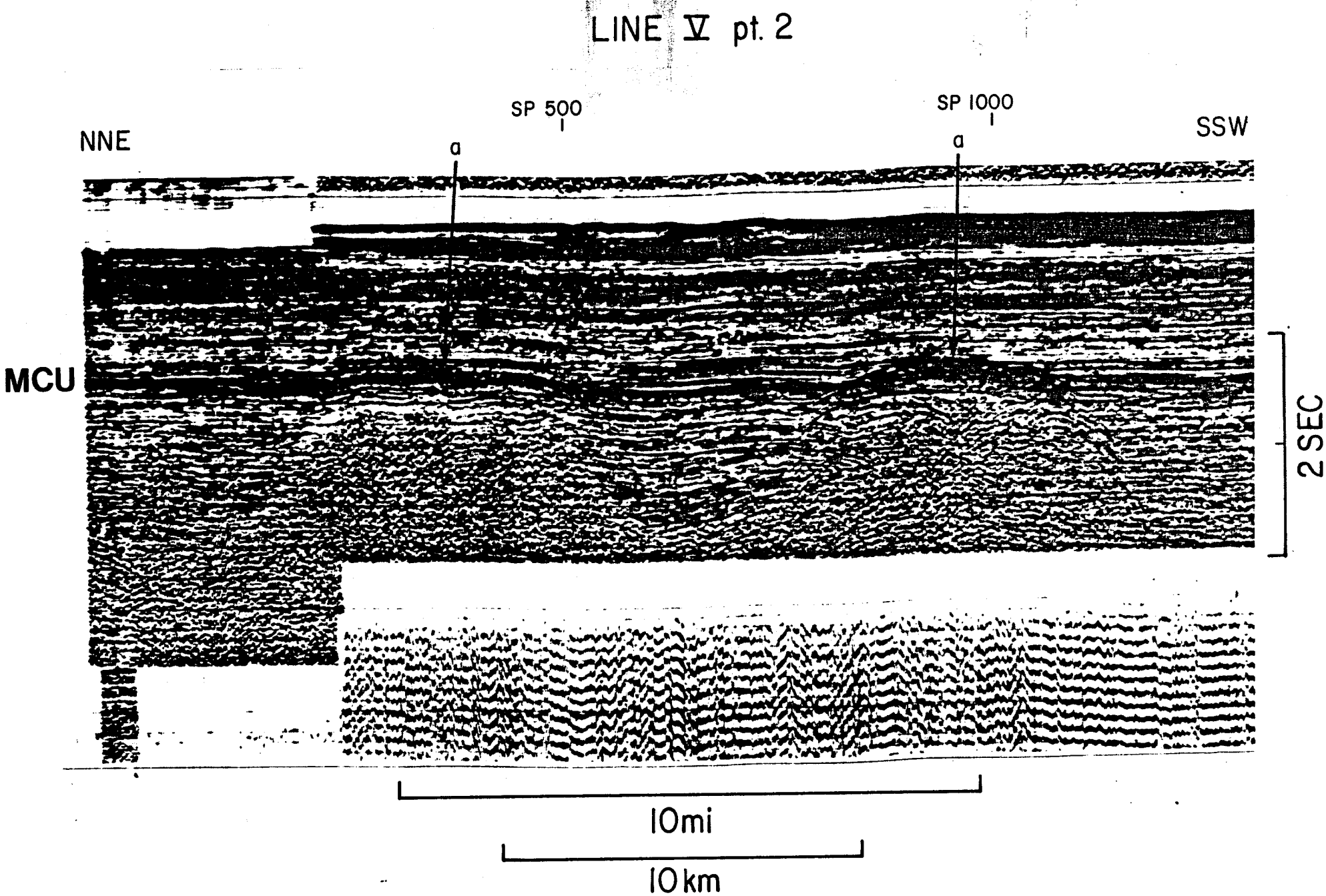

Figure 28

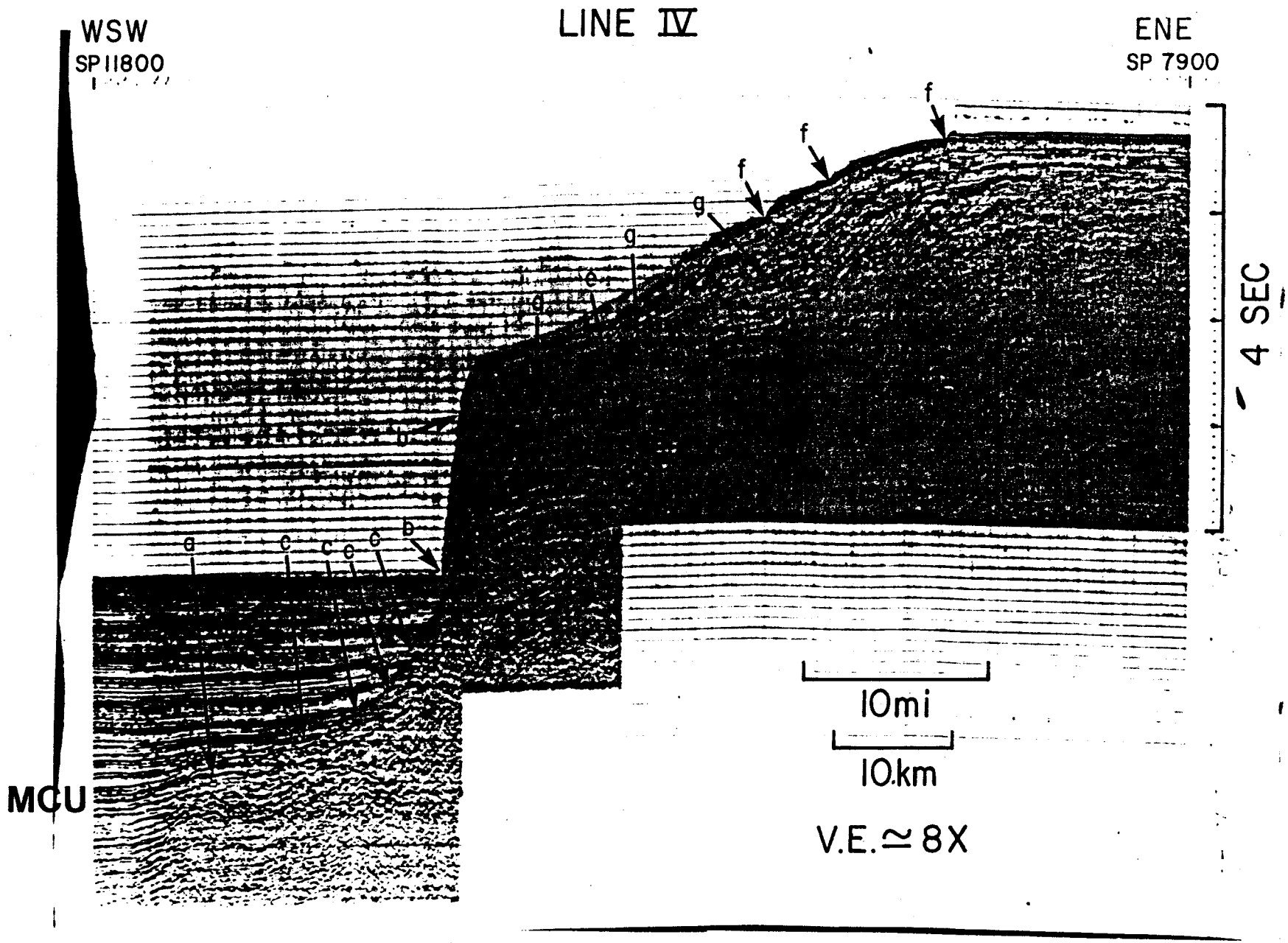
LINE IV
WSW
SP 11800
ENE
SP 7900
f
f
f
g
g
e
d
b
a
c
c
e
c
b
4 SEC
10mi
10km
V.E. ≃ 8X
MCU

Figure 29

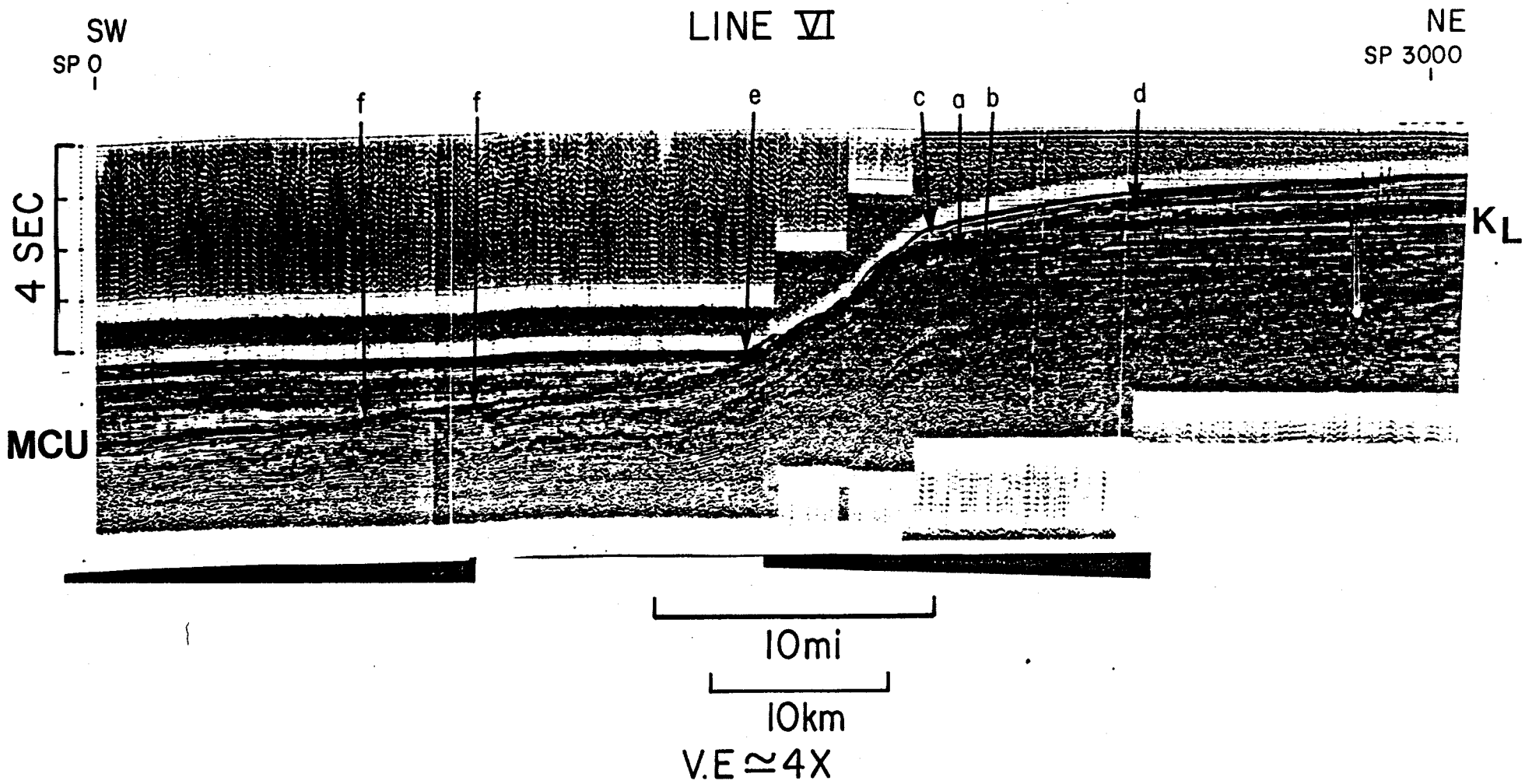

Figure 30

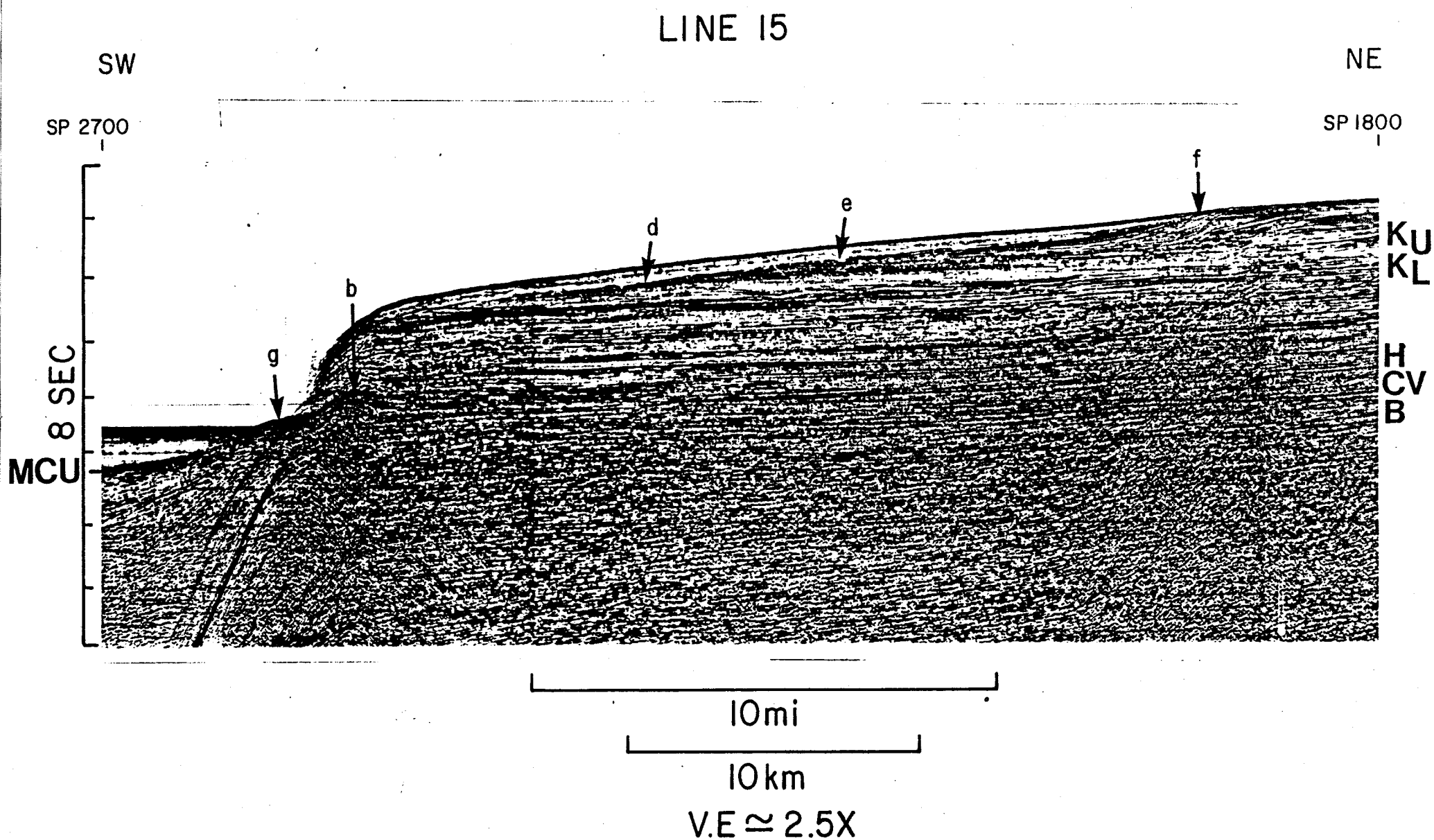
LINE 15
SW
NE
SP 2700
SP 1800
8 SEC
MCU
g
b
d
e
f
KU
KL
H
CV
B
10mi
10km
V.E ≃ 2.5X

Figure 31